NOTICE

The quality of this microform is heavily dependent upon the quality of the original thesis submitted for microfilming. Every effort has been made to ensure the highest quality of reproduction possible.

If pages are missing, contact the university which granted the degree.

Some pages may have indistinct print especially if the original pages were typed with a poor typewriter ribbon or if the university sent us an inferior photocopy.

Reproduction in full or in part of this microform is governed by the Canadian Copyright Act, R.S.C. 1970, c. C-30, and subsequent amendments.

AVIS

La qualité de cette microforme dépend grandement de la qualité de la thèse soumise au microfilmage. Nous avons tout fait pour assurer une qualité supérieure de reproduction.

S'il manque des pages, veuillez communiquer avec l'université qui a conféré le grade.

La qualité d'impression de certaines pages peut laisser à désirer, surtout si les pages originales ont été dactylographiées à l'aide d'un ruban usé ou si l'université nous a fait parvenir une photocopie de qualité inférieure.

La reproduction, même partielle, de cette microforme est soumise à la Loi canadienne sur le droit d'auteur, SRC 1970, c. C-30, et ses amendements subséquents.

Canada

DESIGN OF CONTROLLERS ASSOCIATED

WITH STATIC VAR COMPENSATORS FOR DAMPING OF

LOW FREQUENCY OSCILLATIONS IN A POWER SYSTEM

Ravi Bhushan Kashyap

A thesis

in

The Department

of

Electrical and Computer Engineering

Presented in Partial Fulfillment of the Requirements

for the Degree of Master of Engineering at

Concordia University

Montreal, Quebec, Canada

March 1993

The author has granted an irrevocable non-exclusive licence allowing the National Library of Canada to reproduce, loan, distribute or sell copies of his/her thesis by any means and in any form or format, making this thesis available to interested persons.

L'auteur a accordé une licence irrévocable et non exclusive permettant à la Bibliothèque nationale du Canada de reproduire, prêter, distribuer ou vendre des copies de sa thèse de quelque manière et sous quelque forme que ce soit pour mettre des exemplaires de cette thèse à la disposition des personnes intéressées.

The author retains ownership of the copyright in his/her thesis. Neither the thesis nor substantial extracts from it may be printed or otherwise reproduced without his/her permission.

L'auteur conserve la propriété du droit d'auteur qui protège sa thèse. Ni la thèse ni des extraits substantiels de celle-ci ne doivent être imprimés ou autrement reproduits sans son autorisation.

Canada

ABSTRACT

This thesis is concerned with the development of a supplementary controller associated with a Static Var Compensator for damping of low-frequency oscillations (0.05 - 2.0 Hz) which are normally present in power systems. The objective of this thesis is to demonstrate that with the use of load modulation, damping of intermachine and system oscillation can be increased.

The development of supplementary controllers requires that a simplified model of the system be available. In large systems this can be a difficult process. In this thesis a simplified approach is presented. It is based on fast fourier transform analysis of the response of the system in time domain from which a reduced order transfer function is determined. This analysis is carried out on a system similar to that of Hydro-Québec. Classical control system design methods (root locus and bode plot) are then used to design the controller, limiting the analysis to the linear region. The extent of this region is defined in the thesis.

The design of this controller is carried out and its effectiveness demonstrated in the environment of Matrix$_x$, a mathematical software package. It is then confirmed for the detailed system using in-house transient stability program.

The simulation results show the effectiveness of these controllers to damp the oscillations with the use of locally available variables. It is also shown that these controllers can be used to damp out the oscillations which may not be locally observable on the bus but are made available through the use of remote communication.

ACKNOWLEDGEMENTS

TABLE OF CONTENTS

LIST OF FIGURES

LIST OF TABLES

CHAPTER 1

INTRODUCTION

1.1   Introduction and Background

This thesis is concerned with the development of a design procedure for a stabilizer associated with a static var compensator for damping out low frequency oscillations in a power system, thereby increasing the stability margin. The term stability of any power system can be defined as the ability of the system to return to its original or new operating point following the disturbance. This can be achieved through control of synchronous generators by ensuring that synchronism is maintained between all operating generators during and after the disturbed conditions.

The term stability can be further subdivided into two categories, that is steady state and transient stability. These subdivisions are based on the level of disturbance. If the disturbance is small and the system returns to its earlier state, it can be termed as steady state stable. If the disturbance is large (for example a 3 phase fault with a removal of transmission line) and the system is able to withstand this and return to its earlier operating point or to any new acceptable operating, it can be termed as transiently stable [15]*.

* references have been listed in chronological order as given on page 78 onward

In any power system, power transfer between two voltage sources connected by a pure reactance is given by the expression

$$P = \frac{E_1 E_2}{X} \sin \delta \qquad (1.1)$$

where E_1, E_2 are the voltages of the sources between which power transfer takes place, δ is the angular separation between the two voltage sources and X is the reactance of the interconnecting line over which power flows (refer figure 1.1).

The steady state limit of power transfer occurs when δ reaches a value of 90° and it is defined by the equation

$$P = \frac{E_1 E_2}{X} \qquad (1.2)$$

Machine 1   Machine 2

$E_1 \angle \delta_1$ X $E_2 \angle \delta_2$

$P_{e1} \longrightarrow$ $\longleftarrow P_{e2}$
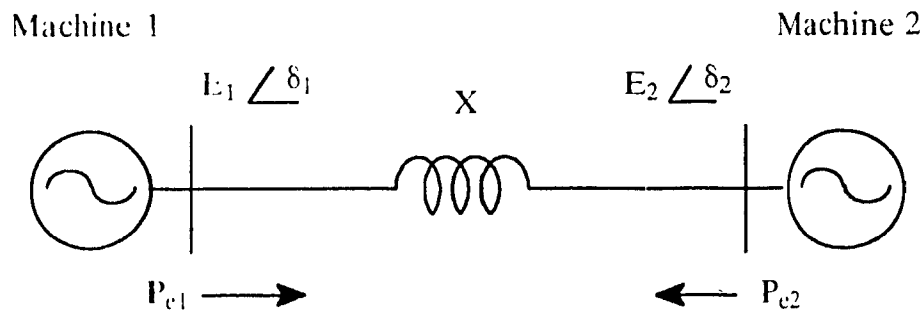
Figure 1.1 Two machine system

The maximum value of δ that is 90° can be exceeded under transient conditions immediately following a disturbance when the electrical power output is different from the mechanical power input. During fault conditions for example a 3phase fault, the electrical power output during the fault drops to zero but the mechanical power is not affected for some time as time constants involved are quite large, thereby resulting in acceleration of the rotors. When the machines are of different

2

sizes this results in the increase of the angular separation $(\delta_1-\delta_2)$. If the fault is cleared within a certain time period, the electrical power output again rises and the machines decelerate and lose the kinetic energy accumulated during the period of the fault. The system remains in synchronism if the areas under the curve defined by equation 1.1 for these two conditions are equal.

It can be observed from the power flow equation 1.1 that the control on power swings in steady state and transient conditions is dependant on voltage levels E_1 and E_2 and angular separation $(\delta_1-\delta_2)$ between the two machines. The line reactance X can be assumed to be constant for this analysis. Introduction of change in the relative angle δ involves changes in the speed of the prime movers attached to the generators. The prime movers used in this study are mostly of the hydraulic type where speed changes can be affected only through control of gate position which regulates the amount of water flow into the turbine, this usually involves time constants of the order of few seconds.

Controlling the power swing by voltage control action can be very fast through the use of fast acting control devices for reactive power compensation such as static var compensators (SVC), synchronous condensers etc. This can be shown with the help of a system similar to as shown in the figure 1.1 except for a SVC is placed in the middle of transmission line(refer figure 1.2). This midpoint point voltage can be defined as E_M. By rapidly controlling the reactive power at the midpoint, the SVC can control E_m and maintain it equal in magnitude to E_1 and E_2, the required power flow between the two buses E_1, E_m and E_m, E_2 can then be achieved with half the angular difference.
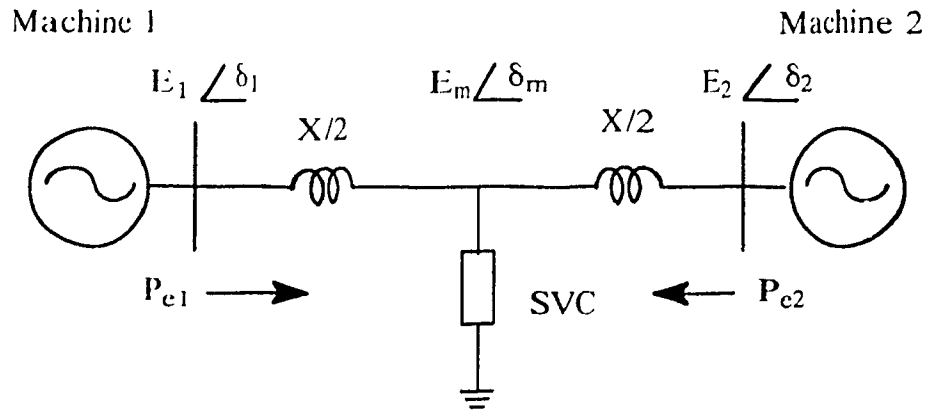
Figure 1.2 Two machine system with SVC

This reduction in the angular separation makes the system more stable as enough margin is available to the two machines to remain in synchronism during and in the time period following the disturbance.

The other important factor in power system stability is damping. After the disturbance has been cleared the generators tend to oscillate about the pre-fault or new operating conditions in order to find a balance between input mechanical power and output electrical power. Large groups of machines may oscillate together or there can also be interactions between two group of machines in different locations. These oscillations result in oscillations of voltage, power and frequency and are unacceptable if they persist for a long time.

In order to effectively damp out these oscillations, special stabilizers have been installed in fast acting excitation systems of generators. Similar type of stabilizers are being proposed for use with fast acting static var compensators also.

1.2   Review of Literature on SVC Control of Power Systems

In this section, review of some existing literature describing the use of SVC and its stabilizing controller for improving the system damping, transmission capacity and transient stability is carried out.

For any system with n machines, there are n−1 modes of oscillation associated with it [48, 54]. These modes are generally well damped and appear for only a few cycles following a disturbance or a fault. However, if some of these modes become less or negatively damped because of a change in system configuration or operating condition, it can pose a serious problem to system stability. Further, in view of the many interconnections expected in the near future, the requirement to increase damping has become more of necessity for stable operation[45].

Initial work on stability was carried out by Hefforn and Phillips[1] and they proposed for analysis purposes a system model represented by one machine connected to an infinite bus . Concordia and de Mello[2] utilized this approach for determining the stability criteria for different operating conditions.

Reactive power compensation as a means for increasing the system damping has been recognized by many authors [23, 29, 30]. SVC's are one of the control devices which are being used to provide reactive power very quickly when needed. D. McGillis et al., [7] and R. Elsiger et al. [8], looked into the importance and optimisation of SVC's for the Hydro-Quebec system. L. Gerin Lajoie et al., [56] studied the application of several SVC's to Hydro-Quebec system using eigenvalue technique.

L. Gyugi [9, 25] presented the importance of SVC on voltage control and thereby increasing the transmission capability of the system The use of the supplementary controller is also stressed to improve the system damping require-

ments. It was highlighted in the paper that an SVC with only voltage control loop will not be able to damp out the low frequency oscillations and a supplementary controller is necessary.

E. V. Larsen et al. [28], showed the interactions between SVC parameters and system strength. Various cases were discussed and the effect of Power system characteristics and strength on SVC transient response was demonstrated. The authors highlighted that the voltage regulating loop of the SVC can, under certain conditions (based on system strength and its parameters), become unstable leading to undamped oscillations. The effect of various load models on system damping was studied using a two-area system. The choice of input signal was studied using controllability and observability factors. The signals highlighted were frequency of ac voltage, current or power flow on a tie-line, voltage magnitude. A design of damping controller was suggested and was tested on the two and three area system with different signals as input.

A. E. Hammad [17,19, 26] presented the applications of using a SVC for stabilizing power systems. It highlights that constant voltage control of the SVC limits its capability to enhance the damping power. Analysis was carried out using eigenvalue techniques on IEEE benchmark system and control action based on bang-bang operation of SVC was suggested. It was also pointed out that the signal proportional to rate of change of power or δ may not be able to provide the necessary damping in certain cases.

A. Olwegard et al., [10] showed that the thyristor controlled reactive power can be used as an efficient tool to improve the system damping. The network studied was Nordel system which consists of national system of Sweden, Finland and Denmark. Control strategies were developed based on switching of capacitor banks dependant on the rate of change of power flow in the lines.

Ohyama et al., [21] presented that in view of complex power transmission networks and heavy load characteristics, it becomes necessary that the SVC be also utilized to improve the system damping. The authors propose to apply a technique called as "Reset filter" which is added to voltage determining circuit of the SVC. This Reset Filter will contribute in increasing the damping torque. Analysis was performed based on eigenvalue analysis and time domain simulations on a sample system. The results presented showed that the employment of reset filter makes SVC more effective to damp oscillations.

The power system is a nonlinear system and for analysis in most of the literature discussed above, use is made of equivalent comprising of two machine or one machine connected to infinite bus. J. F. Hauer [16] proposed the use of fitting structured models to measured frequency response of the system. It was presented in the paper that with the help of some computer routines developed at Bonneville Power Administration (BPA) system models were identified and developed in the frequency domain to represent a linear model of power system for their use in digital filter and controller design applications.

Analysis of time domain outputs from transient stability programs or from actual field results is an another possibility for identification of reduced order models of the power system. K. P. Poon and K. C. Lee [32] presented the use of Fourier transformation to analyze the transient stability swings of a interconnected system. In this method the frequencies of interest are identified individually using fourier transformation and their damping constants are obtained by comparing the magnitudes of different frequencies in several time windows. The results of some test cases were compared with the linear eigenvalues analysis and good correlation was observed.

7

J. F. Hauer et al. [35, 36, 45] presented the use of Prony analysis for analyzing the outputs of transient stability programs and actual field results. This method could be used directly to determine the frequency, damping, strength and phase of modal components present in the signal. This method was applied to model the results of a brake pulse applied to Pacific AC intertie exporting power to Pacific Gas and Electric. The system as identified by this method gave a good fit to the original signal obtained from field results. The use of Prony method was further extended by D. J. Trudnowski et al. [42]. The authors used this method to determine a reduced order model for a sample system comprising of 27 buses and 16 machine system. The system was a simplified representation of western North American power system. With the help of reduced order model and root locus technique a power system stabilizer was designed at one of the machines in order to effectively damp out the interarea oscillations.

1.3   Problem Description and Scope

In the present thesis, the design of system stabilizers associated with static var compensators is examined and a demonstration is made that such stabilizers can be effective for the damping of system oscillations. In chapter 2 the theoretical basis for the feasibility of such stabilizers is briefly examined.

Power systems in general are non-linear in their behavior. However it is shown that within an important range of interest they can be considered to be linear and therefore classical techniques developed for control of linear systems can be used for the design of the stabilizers.

The first step in the design procedure is the definition of the system under study and its model as viewed by the stabilizers. Power systems are very complex

and of very high order with hundreds of buses, different types of loads, and many types of generators with their prime movers, voltage regulators etc. Furthermore they are interconnected to other systems and therefore finding a linearised model based on the knowledge of its components, would be practical.

The system total generation and load is another factor which is varying periodically, it can change depending on the season e.g. average load in summer is different than average load in winter. The load condition may also vary during part of the day and specially in the mornings when the load change can be as fast as 100 Mw/min for some power systems [15a]

Considering the above, the approach adopted here is to identify the system as an equivalent reduced order model obtained from examining its response to an impulse function. The behavior of the system after the disturbance by the impulse function is studied through simulation using a transient stability program.

The model so obtained is then used to design the compensator associated with one of the SVC existing in the network.

1.4   Organization of Remaining Chapters

The following sections are organized into five chapters. Chapter 2 is further subdivided into two parts. The first part contains a preliminary theoretical analysis of the effect of load modulation on intermachine swings. The second part of this chapter analyses the criteria for chosing the most suitable location of SVC(for damping of low frequency electro-mechanical oscillations) in a power system. Chapter 3 describes the system identification process for finding the reduced order model of the system. The model identified is validated with the help of general purpose mathematical software matrix$_x$. Chapter 4 contains the design procedure used for designing the supplementary controller in the matrix$_x$ environment. The design is finalized with the help of root locus technique and simulation results . Chapter 5 describes the integration of this supplementary controller to the transient stability program. The confirmation of the design procedure is carried out by comparing the simulation results before and after the controller being put into service. Chapter 6 presents a brief discussion on the conclusions and aspects requiring future work.

CHAPTER 2

THEORETICAL ANALYSIS AND SYSTEM DESCRIPTION

2.1   Introduction

In this chapter a simple system is analyzed to determine the factors that influence inter-machine the intermachine oscillations. The knowledge of these factors is then applied to damp power swings in a network similar to that of Hydro-Quebec.

For a preliminary analysis, the simple system shown in figure 2.1 is studied. It consists of two generators feeding into a load.

Machine 1   Machine 2

$E_1 \angle \delta_1$ $E_2 \angle \delta_2$

$P_{e1} \longrightarrow$ $\longleftarrow P_{e2}$

Z_3 Load
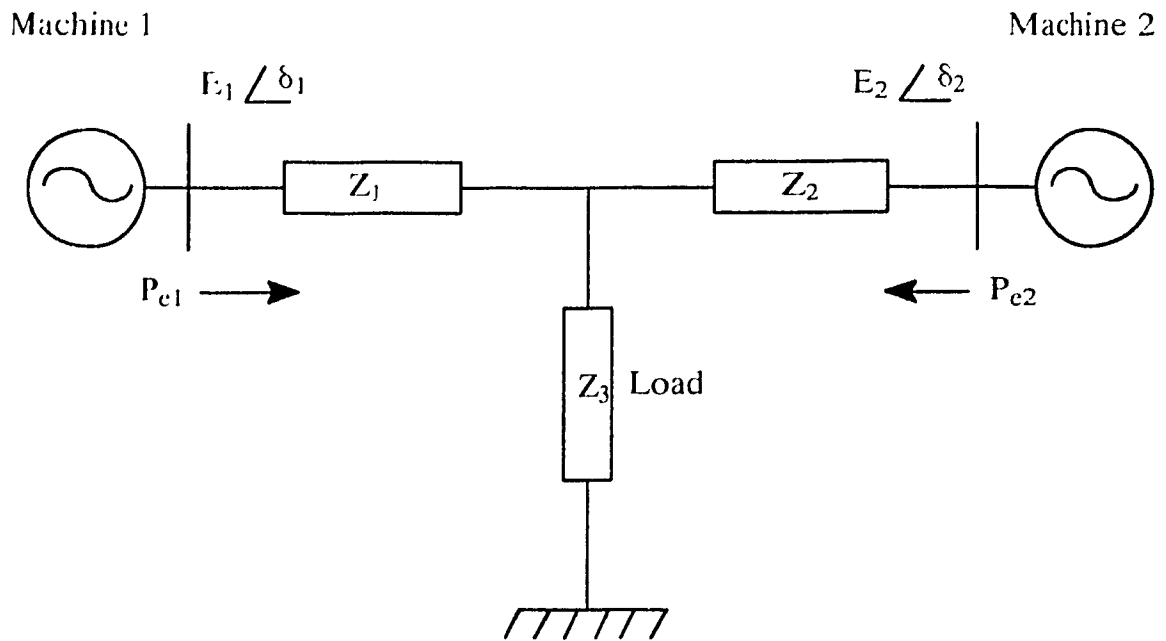
Figure 2.1 Two machine feeding into a load

When such a system is disturbed, machine oscillations are set up. As mentioned in chapter 1, for a system with n machines there are n−1 modes of intermachine oscillations. These can be termed as " intermachine " or " swing "mode. There also exists an n'th mode which represents all the machines acting together as one unit and oscillating about their inertial center [48] against the load. This n'th mode of oscillation can be termed as " system" or " load " mode. The frequencies of oscillations for these two modes (intermachine and load) are quite different. In the load mode the oscillations typically vary from 0.05 Hz to .1 Hz and in the intermachine or swing mode it can vary from a value from 0.1 to 2.0 Hz.

The n−1 intermachine modes are further dependant on many factors. If initially the machines are assumed to be unregulated and of classical model type (constant voltage behind reactance) then these n−1 modes will result in n−1 fixed sim-

ple frequencies. However if the effect of the voltage regulator and the speed governor are included, the system becomes more complex and these n-1 modes are not simple fixed frequencies but are composite of many different frequencies which change with respect to time. For purposes of analysis of machine swings the voltage can be assumed to be constant as the variations are generally small. The oscillations are therefore dependant mainly on the actions of speed governors. The time period after the disturbance can also be divided into two parts. In the first part, which is too small to take into account the action of speed control, the oscillations set up will be natural oscillations, similar to the unregulated case. However for the time period following the start of the actions of governors, the frequencies of oscillations will be quite different from the natural frequencies as described above and will be dependant on the governor characteristics.

In the drawing up of the above conclusions the effects of voltage regulators are neglected. The effects of network conductances, fast acting devices like SVC etc. have also been neglected which may affect the resultant frequencies to certain extent. These two assumptions are assumed for initial basic understanding but have been taken into account for the final design in this study.

Controlled changes in the load will have certain affect on the load mode but it is not evident that they will affect the intermachine mode. One of the objectives of the present work was to study the controllability of both the modes by modulation of the load.

In the system of Figure 2.1 the controllability of the swing mode is examined in terms of the amount of load and its position with respect to the machines.

The electrical power outputs and mechanical power inputs for these two machines are P_{e1} P_{e2} and P_{m1} P_{m2} respectively. Z_1, Z_2 are the impedances between

the load and the two machines: Z_3 is the impedance of the load itself and E_1, E_2 are the voltages at the terminals of the machines.

It can be shown that power output from these machines is given by [55]

$$P_{e1} = \frac{E_1^2}{Z_{11}}\sin(a_{11}) + \frac{E_1E_2}{Z_{12}}\sin(\delta_{12} - a_{12})$$

(2.1)

$$P_{e2} = \frac{E_2^2}{Z_{22}}\sin(a_{22}) + \frac{E_1E_2}{Z_{12}}\sin(\delta_{21} - a_{21})$$

(2.2)

where $\delta_{12} = \delta_1 - \delta_2$ and δ_1, δ_2 are the angular positions of the voltage vectors E_1 and E_2 w.r.t. to a reference axis rotating at synchronous speed:

$$a_{11} = 90 - \theta_{11}$$

$$a_{22} = 90 - \theta_{22}$$

$$a_{12} = 90 - \theta_{12}$$

θ_{11}, θ_{12} and θ_{22} are the impedance angles of Z_{11}, Z_{12}, Z_{22} respectively. Z_{11}, and Z_{22} are the impedances viewed from machine 1 and machine 2 respectively with terminals of the other machine being short circuited and Z_{12} is the transfer impedance. These are calculated as follows :

$$Z_{11} = Z_1 + \frac{Z_2 Z_3}{Z_2 + Z_3}$$

$$Z_{22} = Z_2 + \frac{Z_1 Z_3}{Z_1 + Z_3}$$

$$Z_{12} = Z_1 + Z_2 + \frac{Z_1 Z_2}{Z_3}$$

(2.3)

The bold faced characters are vector quantities, while all other variables and constants not highlighted in bold are scalar quantities.

Considering small perturbations, we have from equation 2.1

$$\Delta P_{e1} = \frac{E_1 E_2}{Z_{12}} \cos(\delta_{12} - \alpha_{12}) \cdot \Delta \delta_{12}$$

(2.4)

$$\Delta P_{e1} = \frac{E_1 E_2}{Z_{12}} (\cos \delta_{12} \cos \alpha_{12} + \sin \delta_{12} \sin \alpha_{12}) \cdot \Delta \delta_{12}$$

(2.5)

Substituting $\cos(\alpha_{12}) = x_{12} / Z_{12}$ and $\sin(\alpha_{12}) = r_{12} / Z_{12}$ in equation 2.5, ΔP_{e1} can be written as

$$\Delta P_{e1} = \frac{E_1 E_2}{Z_{12}} \left(\cos \delta_{12} \frac{x_{12}}{Z_{12}} + \sin \delta_{12} \frac{r_{12}}{Z_{12}} \right) \cdot \Delta \delta_{12}$$

(2.6)

Similarly, for the 2nd machine, ΔP_{e2} can be derived as

$$\Delta P_{e2} = -\frac{E_1 E_2}{Z_{12}} \left(\cos \delta_{12} \frac{x_{12}}{Z_{12}} - \sin \delta_{12} \frac{r_{12}}{Z_{12}} \right) \cdot \Delta \delta_{12}$$

(2.7)

The swing equation which describes the dynamics of a synchronous machine can be written (50)

$$\frac{H}{\pi f} \frac{d^2 \delta}{dt^2} = T_m - T_e$$

(2.8)

where H is inertia constant, δ is the angular position of the rotor of the machine with reference to a reference axis rotating at synchronous speed and T_m, T_e are the mechanical and electrical torques acting on the rotor

The swing equations for small perturbations for the two machines shown in figure 2.1 are

$$\frac{H_1}{\pi f} \frac{d^2 \Delta \delta_1}{dt^2} = \Delta T_{m1} - \Delta T_{e1}$$

(2.9)

15

$$\frac{H_2}{\pi f} \frac{d^2 \Delta\delta_2}{dt^2} = \Delta T_{m2} - \Delta T_{e2}$$

$$(2.10)$$

where the subscripts 1 and 2 identify the two machines 1 and 2 respectively. For small perturbations the terms ΔT_{m1} and ΔT_{m2} can be neglected as the time constants involved in prime movers (hydraulic turbines) are large. On a per unit basis and assuming that changes in speed are small, the change in electrical torque can be taken equal to the change in electrical power, that is, $\Delta T_e = \Delta P_e$.

Applying these assumptions and subtracting equation (2.10) from (2.9), we have

$$\frac{d^2 \Delta\delta_{12}}{dt^2} = \pi f \left(\frac{-\Delta P_{e1}}{H_1} - \frac{-\Delta P_{e2}}{H_2} \right)$$

$$(2.11)$$

$$\frac{d^2 \Delta\delta_{12}}{dt^2} = \frac{\pi f}{H_1 H_2} \left[(\Delta P_{e2} \cdot H_1 - \Delta P_{e1} \cdot H_2) \right]$$

$$(2.12)$$

Equation 2.12 represents the relative acceleration between the two machines and therefore represents the swing mode oscillation. The term $[\Delta P_{e2}*H1 - \Delta P_{e1}*H2]$ can be evaluated with the help of values of ΔP_{e1} and ΔP_{e2} found in equation 2.6 and 2.7.

For the sake of simplicity, it is assumed that

$$Z_1 = jx_1$$

$$Z_2 = jx_2$$

and $\qquad Z_3 = 1$.

To study the changes in load and its position with respect to the machines, two new parameters are introduced

$$a = \frac{1}{(x_1 + x_2)}$$

$$c = \frac{x_2}{x_1}$$

$$(2.13)$$

using $x_1 = x$, we have

$$r = a(1 + c)x \quad \quad (2.14)$$

Substituting the values of c and α from equations 2.13 and 2.14 in equations 2.6 and 2.7 for evaluating ΔP_{e1} and ΔP_{e2}, the term $[\Delta P_{e2}*H_1 - \Delta P_{e1}*H_2]$ can be derived as

$$\Delta P_{e2} * H_1 - \Delta P_{e1} * H_2 = -E_1 E_2 \Delta \delta_{12} \left\{ \frac{1}{x[c^2 + (1 + c)^4 a^2]} [\cos \delta_{12} \, a^2(1 + c)^3 (H_1 + H_2) + \sin \delta_{12} \, ca \, (1 + c)(H_2 - H_1)] \right\}$$

$$(2.15)$$

After further simplification this can be reduced to

$$\Delta P_{e2} * H_1 - \Delta P_{e1} * H_2 = \left\{ \frac{u_1}{x[c^2 + (1 + c)^4 a^2]} [a^2(1 + c)^3] \right\} + \left\{ \frac{u_2}{x[c^2 + (1 + c)^4 a^2]} [ca (1 + c)] \right\}$$

$$(2.16)$$

where $\quad u_1 = -E_1 E_2 \Delta \delta_{12} \cos(\delta_{12}) [H_1 + H_2]$

and $\quad u_2 = -E_1 E_2 \Delta \delta_{12} \sin(\delta_{12}) [H_1 - H_2]$

Multiplying by $(1 + c)$ to both the numerator and the denominator of equation. 2.16 we have

$$\Delta P_{e2} * H_1 - \Delta P_{e1} * H_2 = \left\{ \frac{u_1 (1 + c)}{(x_1 + x_2) [c^2 + (1 + c)^4 a^2]} [a^2(1 + c)^3] \right\} + \left\{ \frac{u_2 (1 + c)}{(x_1 + x_2)[c^2 + (1 + c)^4 a^2]} [ca(1 + c)] \right\}$$

$$(2.17)$$

The two terms on the RHS in the equation 2.17 can be further subdivided into two parts each. One part which is dependant on the amount and the position of the load in the system (that is dependant on variables a and c) The second part which is independent of load. To simplify this, two new variables f_1 and f_2 are intro

duced. These two variables represent the part which is dependant on α and c and are defined in equation 2.17a.

$$F_1 = \left\{ \frac{(1 + c)}{[c^2 + (1 + c)^4 \, \alpha^2]} [\alpha^2(1 + c)^3] \right\} \quad \text{and}$$

$$F_2 = \left\{ \frac{(1 + c)}{[c^2 + (1 + c)^4 \, \alpha^2]} [\alpha c(1 + c)] \right\} . \tag{2.17a}$$

The equation 2.17 can now be written as

$$\Delta P_x \cdot H_1 - \Delta P_{c1} \cdot H_2 = \left\{ \frac{u_1}{(x_1 + x_2)} \cdot F_1 \right\} + \left\{ \frac{u_2}{(x_1 + x_2)} \cdot F_2 \right\} \tag{2.18}$$

In the equation 2.18 the terms $\frac{u_1}{x_1 + x_2}$ and $\frac{u_2}{x_1 + x_2}$ are independent of the load amount and its position. The values of F_1 and F_2 are shown plotted in figures 2.2 and 2.3 respectively for varying values of α and c. The value of α is varied from 0.1 to 10 that is from a very high load to a very low load and c is varied from .01 to 100, this being equivalent to the load being moved from very near to one machine to very near the terminals of the other.

To determine the significance of varying α from 0.1 to 10 an example of a 735 kV line is taken with a typical value of X of 0.33 ohms/km. Considering a distance of 1000 kms from each machine to the load, the total reactance of the line is 0.33 * 1000 * 2 = 660 ohms. The range of α from 0.1 to 10 translates into a load range of 8185 MW to 82 MW at 1.0 p.u. voltage. Typical loading for such lines is 2000 MW each. This variation in α is thus equivalent to a load range of 200% to 2%.

18
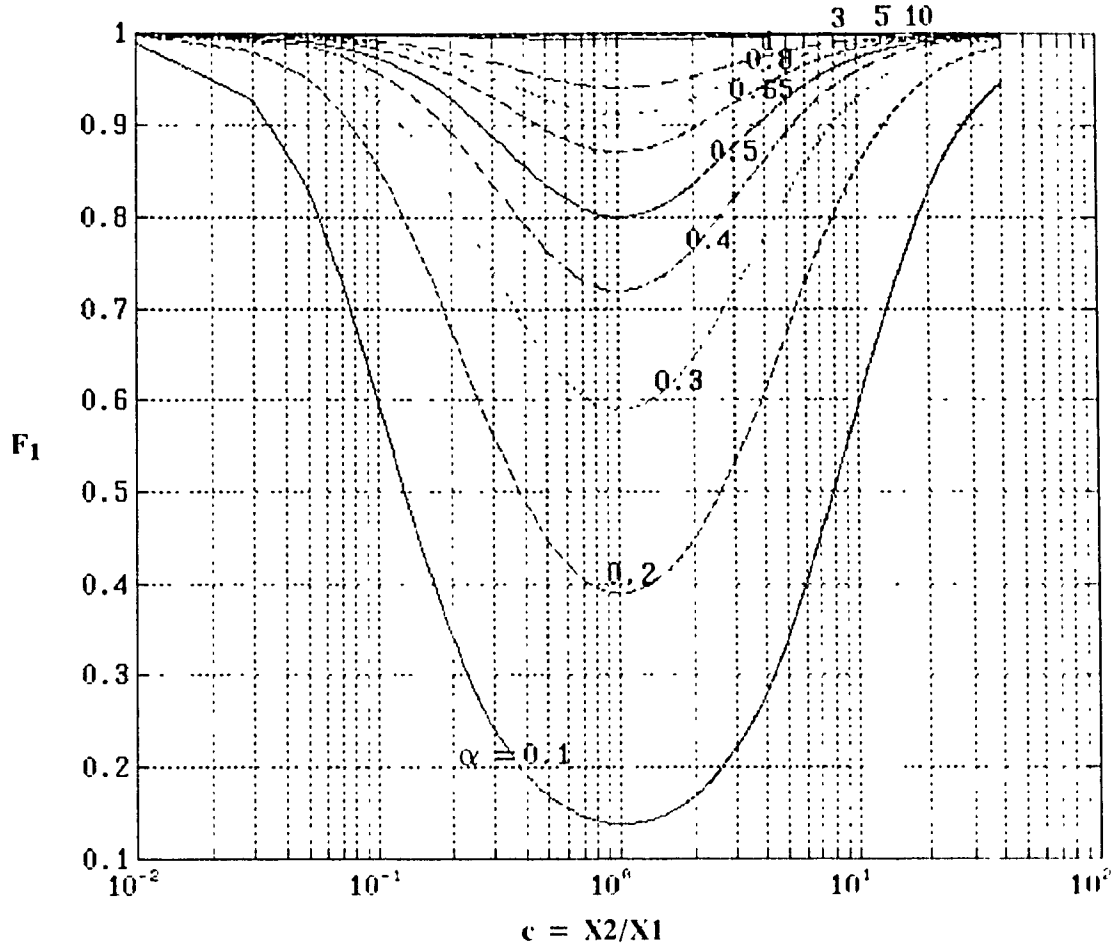
$$F_1 = (\alpha^2 \cdot (1+c)^4) / (c^2 + (1+c)^4 \cdot \alpha^2)$$

Figure 2.2 Plots of variable F_1 vs c for different values of α

Since the expressions $\dfrac{a_1}{x_1 + x_2} \cdot I_1$ and $\dfrac{a_2}{x_1 + x_2} \cdot I_2$ represent the relative acceleration torque it follows that the relative acceleration between the machines or swing mode machine oscillations are dependant on the load and also its position with respect to the machines.

From the figure 2.2 it can be seen that when the value of α is large (corresponding to lightly loaded conditions) the function F_1 becomes independent of

variation in c, however for smaller values of α, the term F_1 varies in a symmetrical manner for increasing values of c.
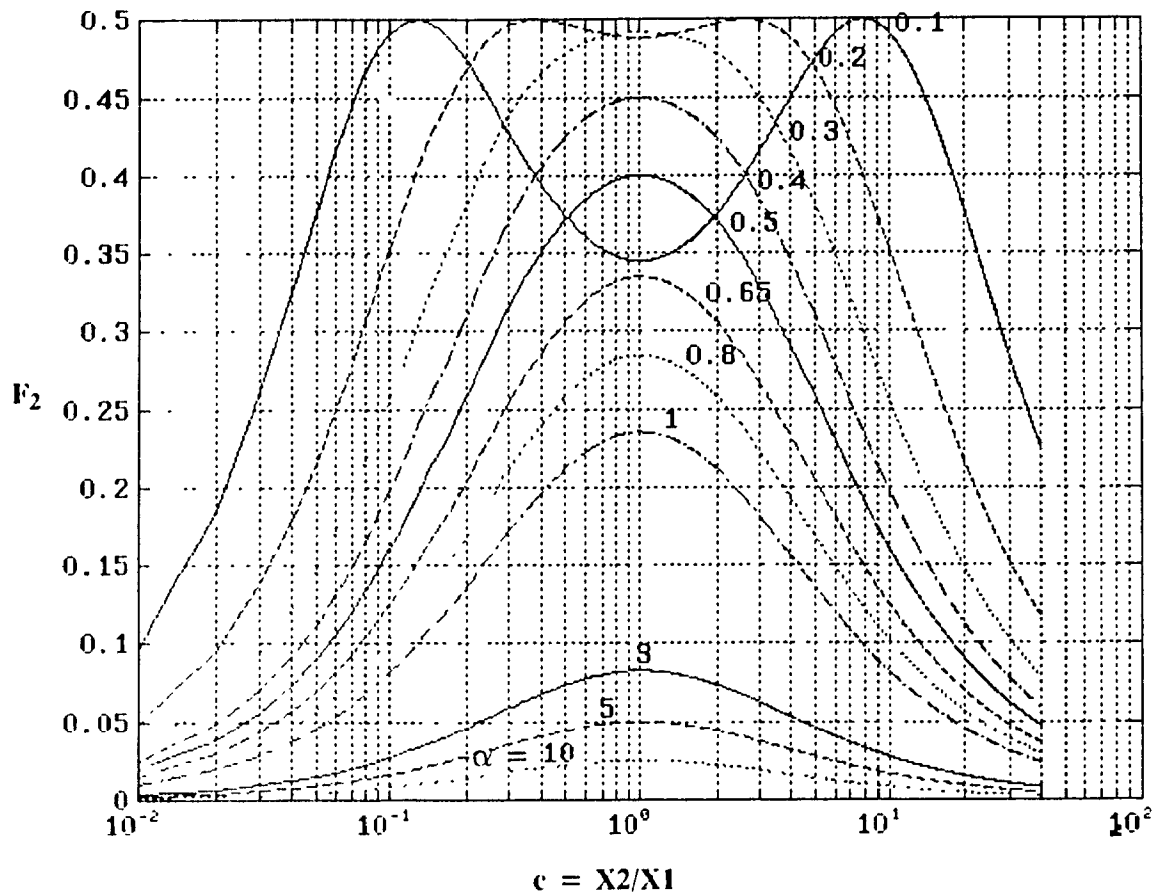
$$F_2 = (c * \alpha * (1+c)^2) / (c^2 + (1+c)^4 * \alpha^2)$$

Figure 2.2 Plot of variable F_2 vs c for different values of α

The function F_2 also varies in symmetrical manner for increasing values of c as shown in the figure 2.3. When c is very low (0.01) or when it is very high value (40), F_2 is nearly zero.
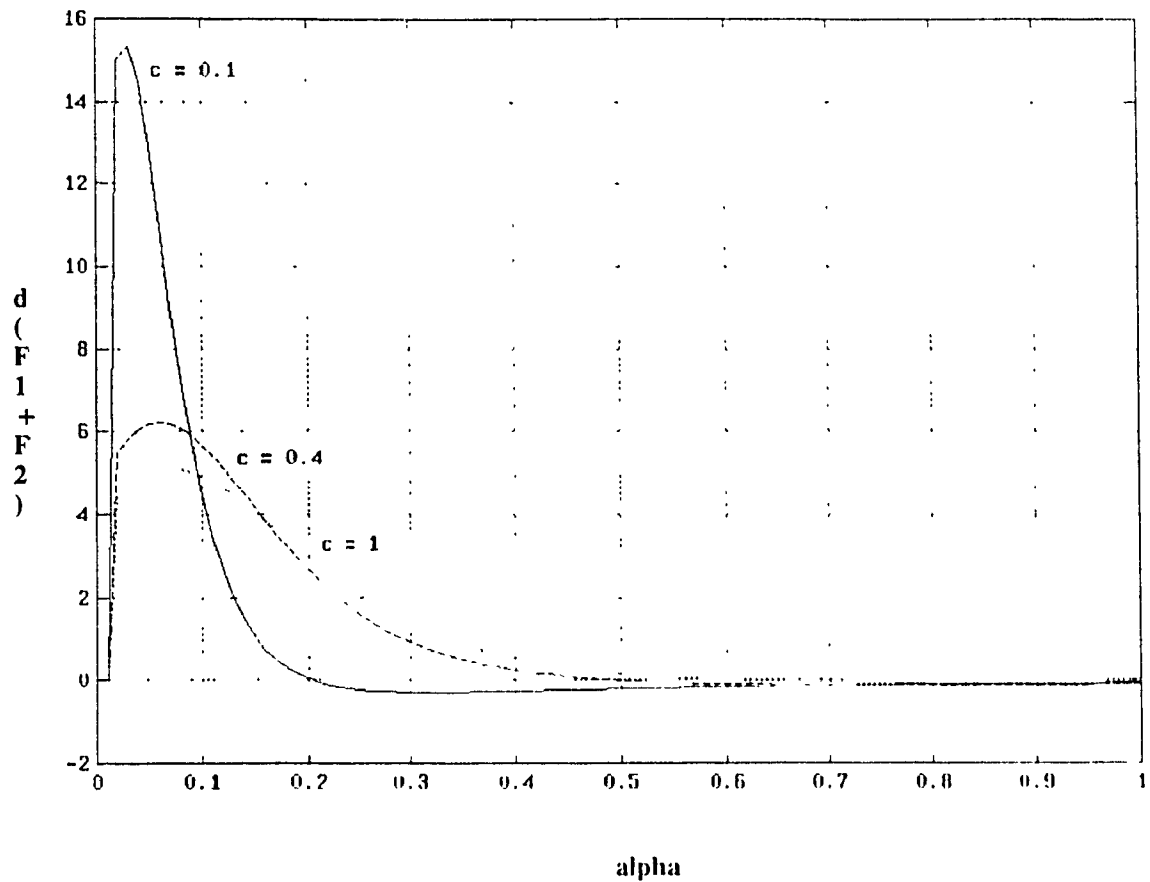
Figure 2.4 Variation of rate of change of $F_1 + F_2$ w.r.t α and c

Figure 2.4 shows a plot of the function $F_1 + F_2$ as also its rate of change with respect to α for three values of c. If we consider d($F_1 + F_2$) /dα as a measure of the controllability of the swing mode then this figure shows that the controllability is maximum at high loads and approaches zero at light loads. At c = 0.1 the controllability is maximum upto value of α = 0.1 but this corresponds to very high loads which might be above the normal operating range and as the value of α is increased it drops very sharply to zero and even goes into negative region. As c is increased towards 1.0 the maxima of the controllability function are reduced but their decline towards zero is slower and if we consider that the normal load corresponds to α = 0.2 then the maximum controllability occurs at c = 1.0 (at the center)

21

From the above analysis two conclusions can be drawn. One, that since the load influences the swing mode oscillations, modulation of load could be used as a means of damping the swing mode and two, that the position of the load with respect to the machines is important and therefore any process of reducing the network must allow for the impedance between each load and the machines. Since no other factor is involved it follows that for the purpose of load aggregation for network reduction, impedance is a sufficient parameter to define electrical distance.

2.2   Load Modulation

One method of modulating the load is to install loads equipped with fast controlling devices, such as thyristor switches, as for example in stored magnetic energy systems. The sole purpose of such special loads is to enhance damping capability of the network.

Another method is to modulate the existing loads by modulating the voltage at the loads since most loads are voltage dependant. This would be in addition to the function of the voltage regulator loop and may be sometimes in opposition to its normal operation. However since the need for system damping is felt most following a disturbance which has in any case introduced some voltage fluctuation, a small determined modulation of the voltage for a short period of time could be acceptable. This method of load modulation would seem particularly attractive for systems which already have voltage regulators placed at a number of points near enough to the loads to influence them.

One such system is the Hydro-Quebec system which has a number of static var compensators, some of which could be used to modulate the voltage to damp the oscillations

For the present study, a system similar to Hydro-Quebec equipped with SVC controllers was chosen and the damping capabilities of load modulation were examined. A sensitivity analysis was first carried out to determine which of the existing static var compensators provided the maximum load voltage variation. This compensator was then selected to introduce the damping control.

2.3   System Description

The system used for this study is similar to Hydro-Quebec 1990 winter network and is shown in figure 2.6. The total generation capacity of this network is about 29,000 MW. There are three major generating centers as shown in the figure 2.6. The power generated at these three centers (22000 MW) is transmitted through two corridors, each comprising five transmission lines, bringing about 2200 MW on each line down to load area. The main transmission system is rated at 735 kV level with sub-transmission at 315 kV. Transmission and distribution below this level is represented by equivalents comprising of loads and equivalent generators as shown in the figure 2.5. The equivalent generator represents the total of local machines with small generating capacities. These machines are assumed to be swinging together during post faults recovery periods. Similarly all the loads below 315kV level were summed up and transferred to the 315 kV busbar.
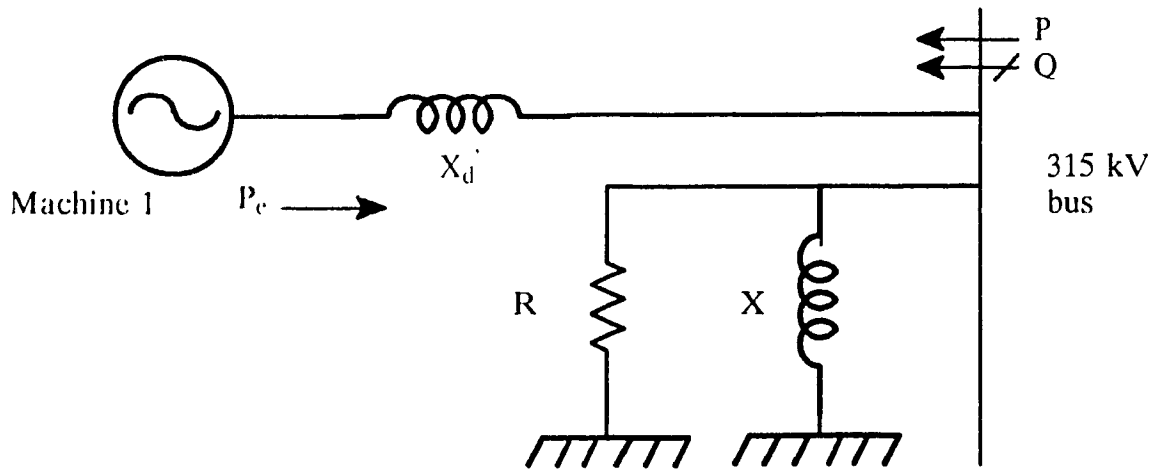
Figure 2.5 A simple representation of the equivalent at 315 kV bus

For the purpose of this study the network was reduced to one having 20 generators, thirty 735 kV, twenty 315 kV busbars and eight buses ranging from voltage level of 230 to 120 kV.

The generator model included the representation of their excitation circuits, stabilizers and turbines.

La Grande

Churchill Falls

LG

CHU

NEM7

CHI7

Legend :

☐ SVC

↓ Major Load Buses

MIC7

LVD7

CHE7

DUV7

JCA7

LID7

LLV7

MAU3

NIC7

CHA7

HER7

BCV7

Montreal and Quebec city Load area

Figure 2.6 Simplified representation of the network

Voltage stability is a very important concern when transferring large amounts of power (2200 MW on each 735 kV line) nearly equal to its surge impedance loading. This necessitates that a voltage profile of near 1 p.u. be maintained at various intermediate points between the generating and receiving ends. All the reactive power generated by long transmission lines is consumed within the line itself during these peak loading conditions, therefore any spare reactive power which may be available for fault recovery in the case of lightly loaded conditions has to be provided by external devices. To provide this necessary support in the HQ network use is made of synchronous condensers and static var compensators. These reactive power devices are designed to provide the support in capacitive and inductive loading. During steady state conditions these voltage support devices are floating on the network with an output of approximately between 0-50 Mvars and they provide the required reactive power support during post fault recovery conditions.

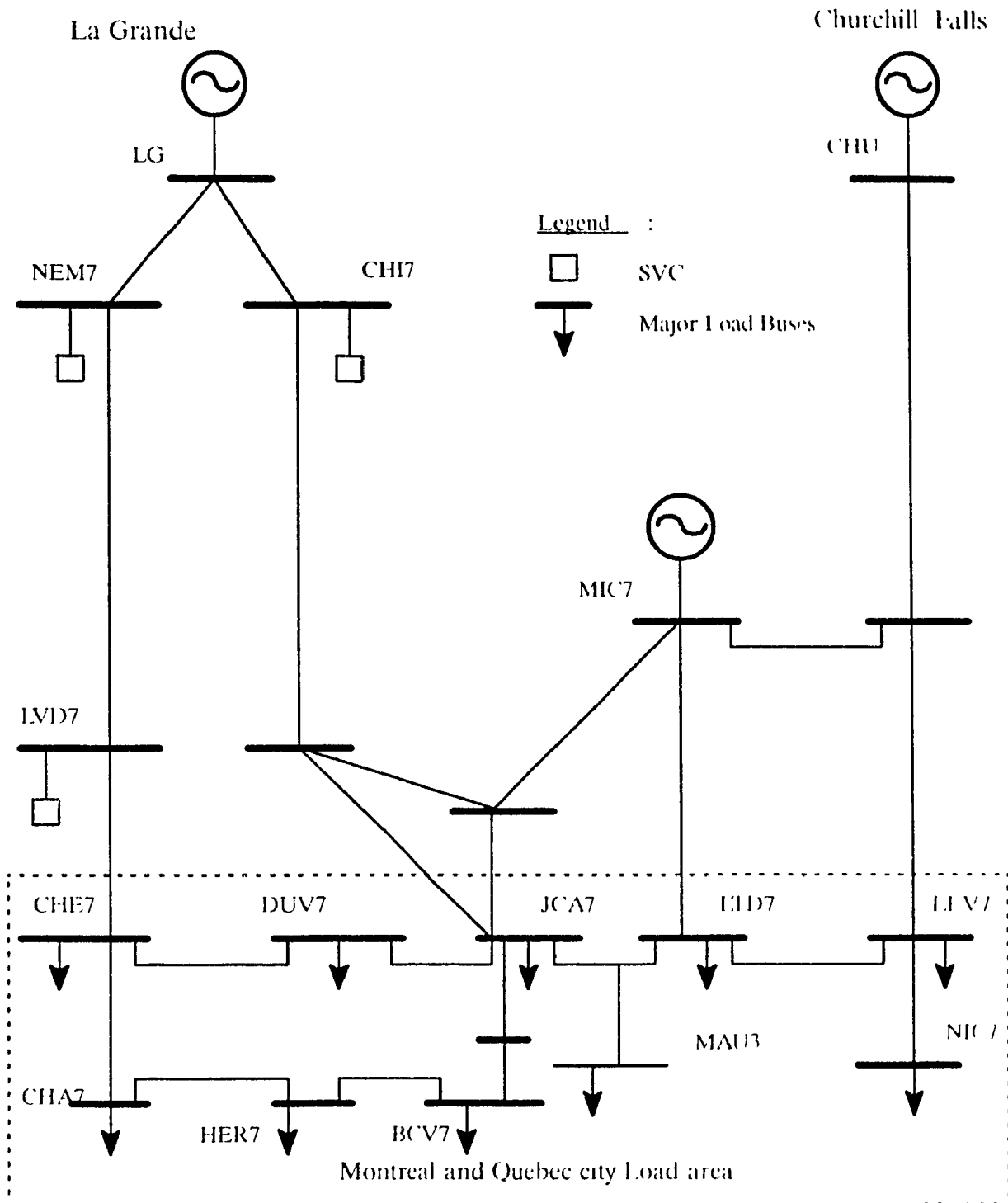The figure 2.6 represents the degraded version of the Hydro-Quebec network. Some transmission lines have also been removed to highlight the oscillations and the effect of the corrective damping method using load modulation.

To illustrate the dynamic response of the system it was simulated on the load flow and transient stability programs of Hydro-Quebec (RP600 and ST600). The load flow program establishes the initial conditions of the network which are then utilized to calculate the dynamic response of the system. A fault of 10 cycles duration was placed on the LVD7 and the voltage and frequency of the system as seen at the bus were recorded for a time period of 30 seconds (1800 cycles) from the simulation using the stability program. These are shown in figure 2.7.

Three static compensators are present in the system at the buses NEM7, LVD7 and CHI7. These SVC's have the primary objective of keeping the voltage con-
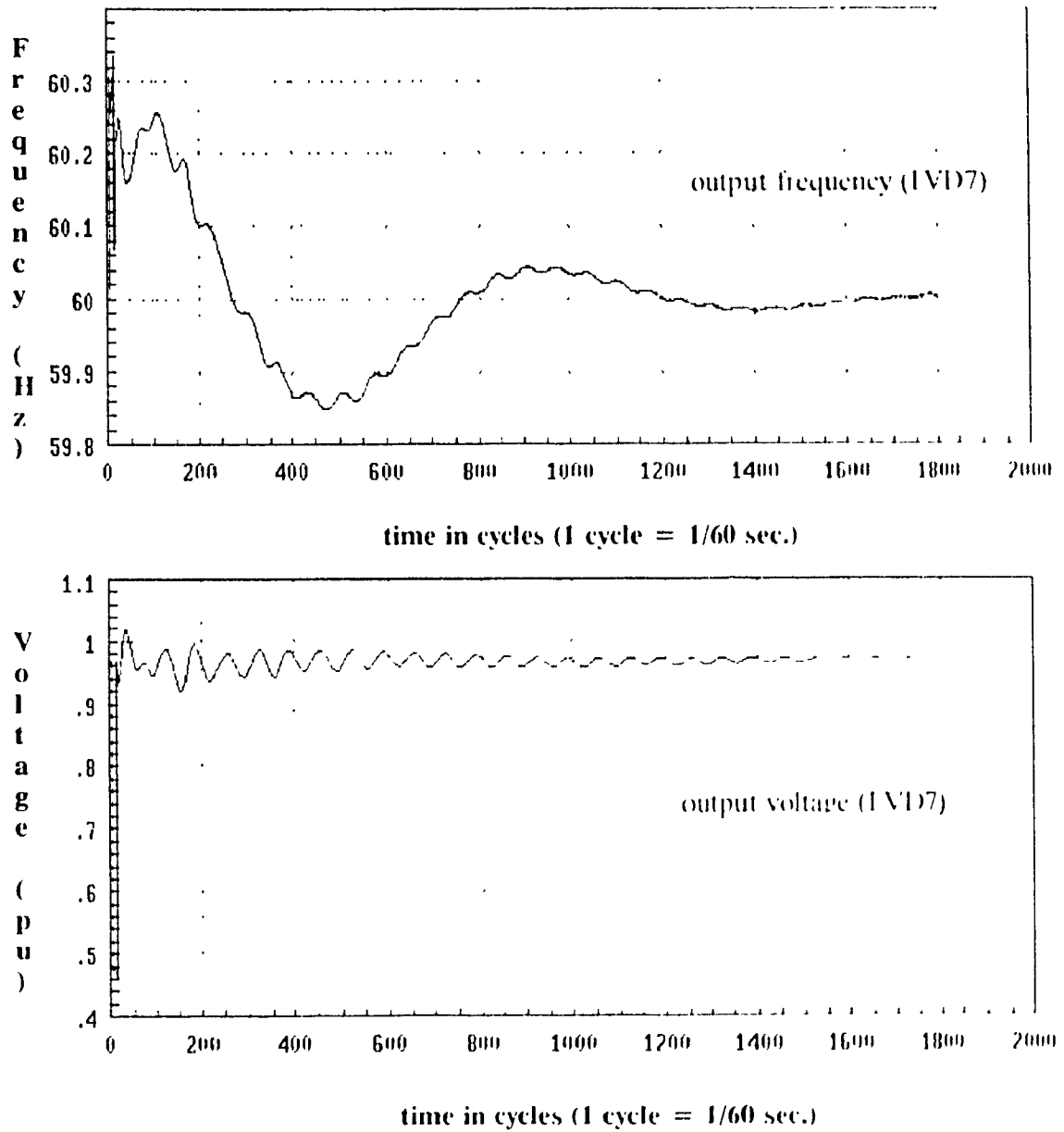
stant on the 735kV busbars.

Figure 2.7   Output waveforms for fault at LVD7 showing the dynamic response of

the system under study.

2.4   Choice of Control Bus

The basic approach to damp out the various mode of oscillation is to modulate the load voltage.
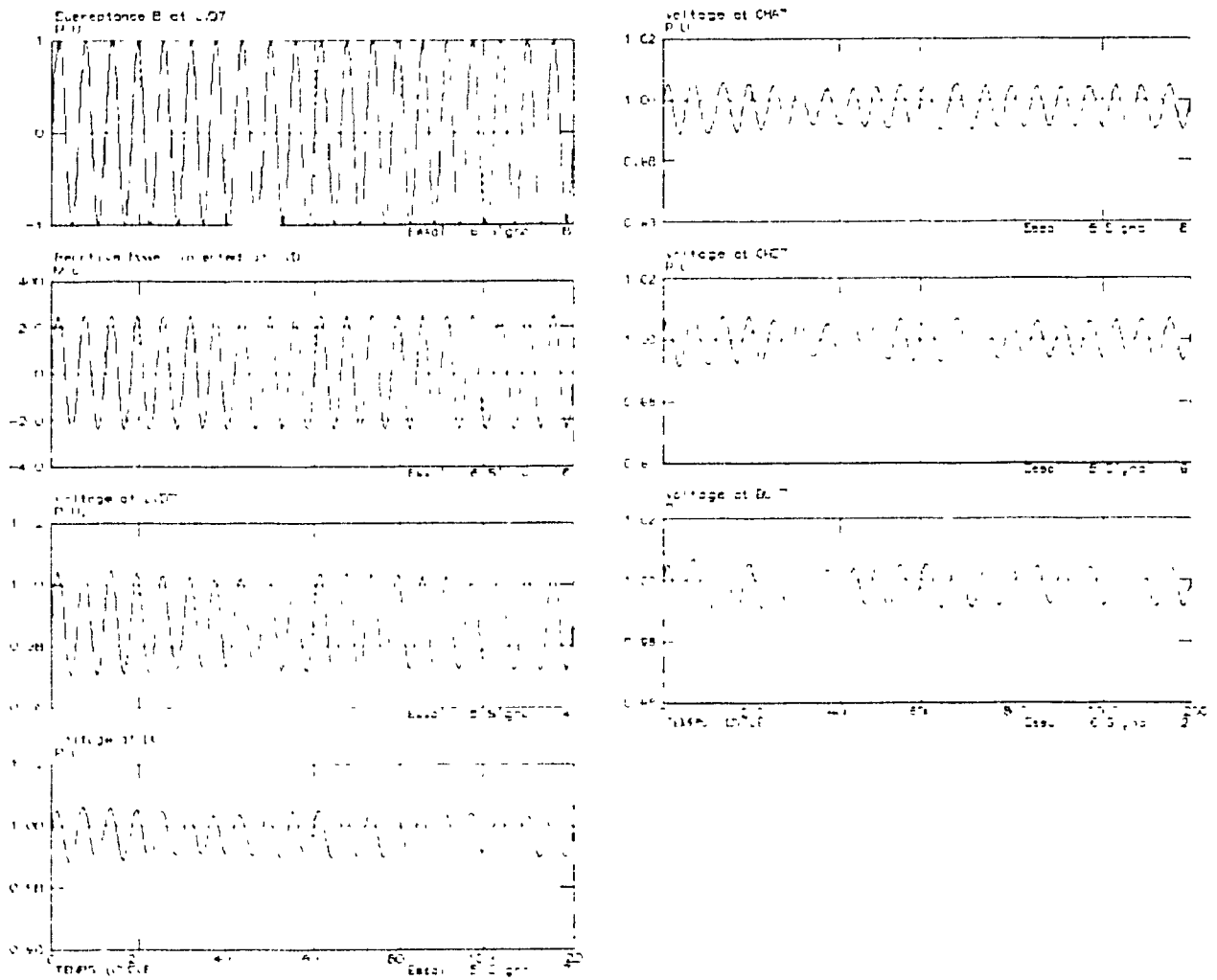
Figure 2.8   Affect of susceptance variation at LVD7 on voltage of important load buses. (1 cycle = 1/60 sec.)

In order to determine which one of the three SVC's mentioned above is most suitable for load voltage modulation, the following simulation study was carried out.

Sr No.	Load Bus	Load MW	Modulating SVC					
			NEM7		LVD7		CHI7	
			V_{max}/V_{min}	ΔV^{2*} Load	ΔV	$\Delta V^2 *$ Load	ΔV	$\Delta V^2 *$ Load
1	DUV7	2838	0.9999/ 0.9938	34.62	1.0046/ 0.9897	84.29	1.0003/ 0.9937	39.73
2	CHA7	2039	1.0003/ 0.9945	23.65	1.0046/ 0.9905	57.30	1.0007/ 0.9942	26.51
3	HER7	2008	1.0027/ 0.9966	24.09	1.0065/ 0.9933	53.01	1.0032/ 0.9964	27.32
4	BCV7	2704	1.0011/ 0.9949	33.53	1.0048/ 0.9916	71.39	1.0015/ 0.9947	36.77
5	CHE7	2011	0.9951/ 0.9892	23.53	1.0011/ 0.9837	69.38	0.9956/ 0.9889	26.75
$\Sigma \Delta V^2 *$ Load				139.42		335.37		157.08

Table 2.9 Affect of variation of B on load modulation showing that the aggregate of load voltages is most sensitive to the svc at the LVD bus.

A slow frequency change in susceptance (1Hz sine wave) corresponding to a magnitude of 250 MVAR was introduced at each of the SVC buses one at a time Voltage variations were recorded at five major Load buses representing about 11600

MW. The waveforms for a typical case, when voltage modulation was applied at the SVC placed at the LVD7 bus, are as shown in the figure 2.8.

The values of maximum and minimum voltages were averaged over 1200 cycles and are as shown in table 2.9. This change when multiplied with the load on each busbar gives a factor which indicates the influence that the SVC can exert on changing load and thereby damping out the electromechanical oscillations. From the table it can be clearly observed that the SVC located on the busbar LVD is able to influence the load around two times more than other SVC's present on the system.

The SVC at LVD7 was therefore chosen for introducing a supplementary control loop to modulate the voltage for damping purpose.

2.5   Controllability and Observability

Various simulations of the chosen system have revealed the presence of dominant mode at 0.068 Hz and three swing modes at 0.55, 0.88, 1.24 Hz. With reference to the figure 2.6 these swings occur between LG and CHU (0.55 Hz), MAU and LG or CHU (0.88, 1.25 Hz). All of these modes can be observed in the frequency signal except for the 0.55 Hz mode, the value of which is too small to be noticed in this signal. To damp this mode its observation will have to be sought in a separate signal. For the purpose of demonstrating the feasibility of damping this mode the angular separation between LG and CHU was used although it is recognized that this has the disadvantage of being dependent on remote sensing.

In order to facilitate the design procedure a reduced order model of the system is derived in the next chapter followed by the design of the controller in chapter4.

CHAPTER 3

SYSTEM IDENTIFICATION

3.1 Introduction

In order to design and optimize the supplementary loop of the static compensator it is essential to know the transfer function of the system as viewed by the compensator, that is, to know the response of the system in terms of voltage and frequency to changes in the reactive power introduced by the compensator at the bus

The system being used for this study is a large power transmission system and although reduced, is still very complex. Deriving the transfer function from a knowledge of its components would be impractical. In view of this it was decided to determine the transfer function of the system by simulation of the system.

For a linear time invariant system the transfer function can be given as

$$G(S) = Y(S) / X(S) \qquad (3.1)$$

where Y(S) is the laplace transform of the output and X(S) is the laplace of the input. The output Y(S) can be expressed as

$$Y(S) = G(S)^* X(S) \qquad (3.2)$$

If the system is excited by a unit impulse whose Laplace transform is 1 then equation 2 can be written as

$$Y(S) = G(S) \qquad\qquad (3.3)$$

which implies that the Laplace transform of the output of the system can be taken as the transfer function of the system. The transfer function as described above contains all the necessary information on the system dynamics.

In a real system the application of a true impulse can be difficult but a pulse may be used instead provided its width is significantly small compared to the smallest time constant of the system.

In the present study, the system was simulated on the transient stability program ST600. A pulse of susceptance was applied at the bus of interest and the response was recorded in terms of voltage and frequency at the bus. The duration of pulse was 0.167 seconds. The test was repeated for a number of values of the susceptance, that is, varying the height of the pulse for different cases.

3.2   Linearity of the system :

The responses of the system to different pulses ranging from susceptance B equal to 10 to B equal 334 p.u. are shown in the figure 3.1
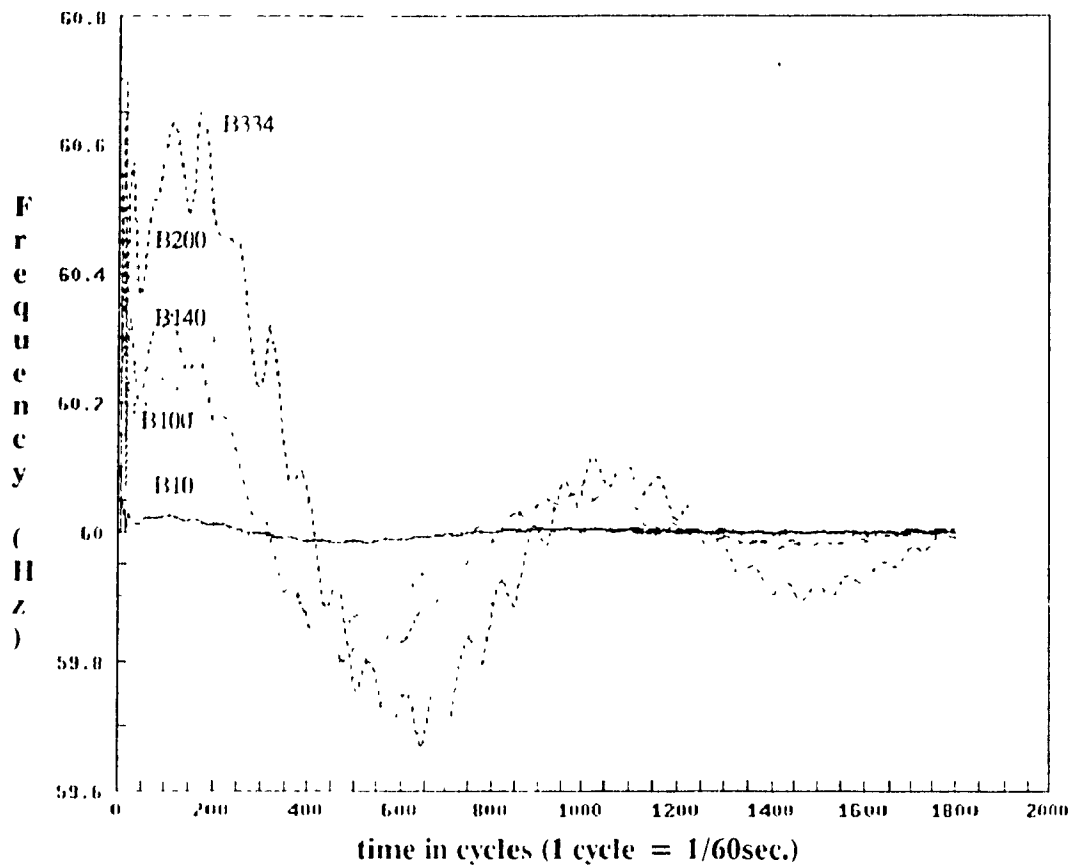
Figure 3.1 Output frequency at LVD7 for pulses of B (different strengths)

Taking the maximum deviation of the frequency as a measure, it can be observed that the response is not uniformly proportional to changes in B. The response for value of B equal to 100 p.u. (B100) is indeed 10 times the response for B equal to 10 p.u. , but this linearity is not maintained for all values of B. Using the response of B100 as 1.0 p.u. the frequency deviations for different pulses are plotted in the figure 3.2. Only the lowest frequency component (0.0683) of each response is considered for this purpose

34
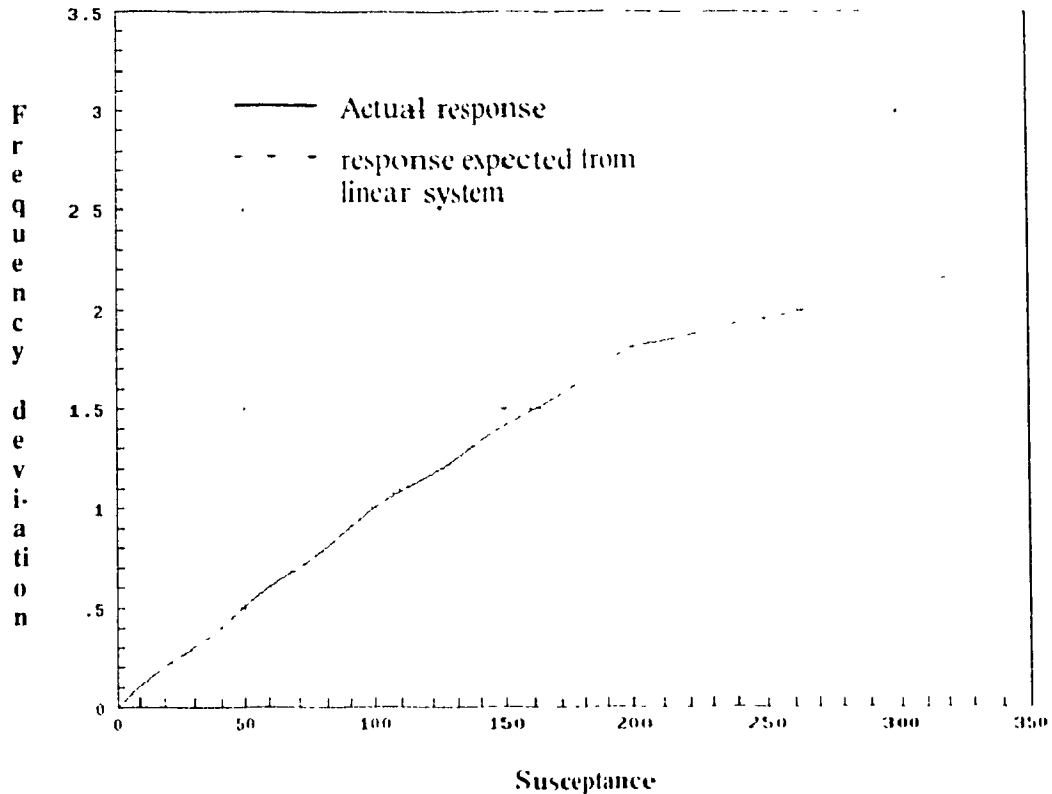
Figure 3.2 Maximum frequency deviation w.r.t pulse height

From the figure 3.2 it can be concluded that the system may be considered linear for changes in susceptance pulses of heights less than 100 (p.u.). This corresponds to voltage drop (during the time period of the pulse) of 50%.

The change in relative phase of the dominant frequency component is also an indication of nonlinearity. Figure 3.3 shows graphs with response for B100 as reference, from which it can be observed that as the susceptance is increased the phase difference between the two curves increases. However the basic mode of oscillation remains the same as obtained by FFT analysis performed on the output frequency This is shown in the figure 3.4.
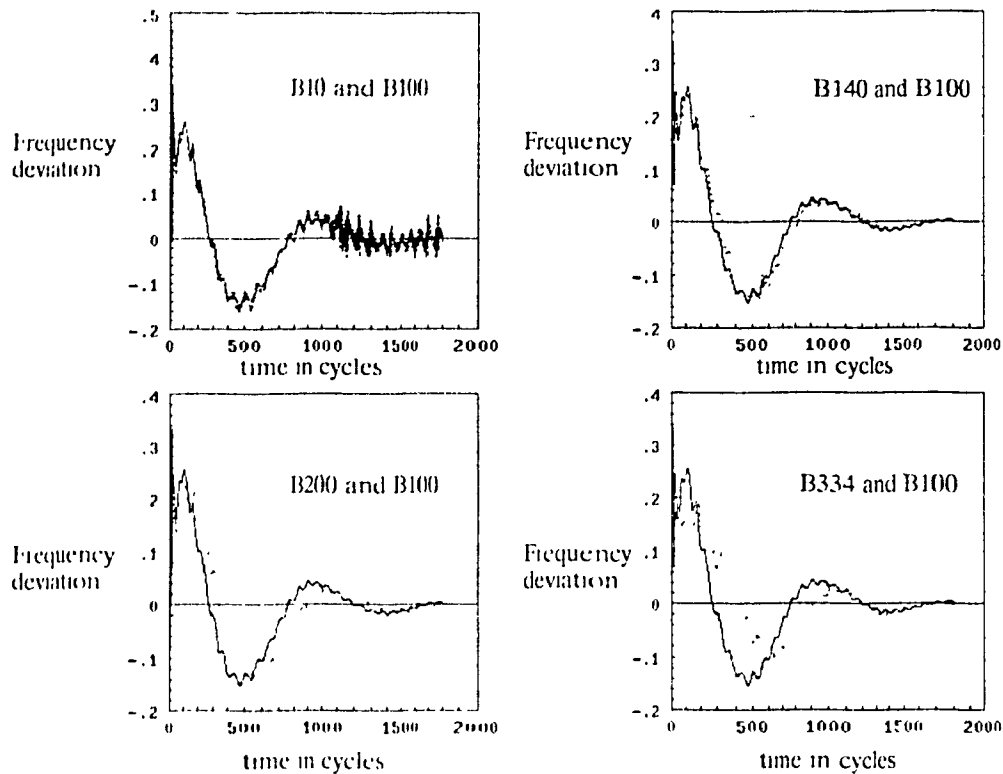
Figure 3.3 Plot of frequency deviations for different disturbances(pulse

height) showing the shift in phase with reference to the case of B100

The pulse width was same in all cases = 10 cycles.(1cycle = 1/60 second)

In any practical system, although the variation in voltage following a fault or other major perturbation can exceed 0.5 p.u., the fault is removed very rapidly and it is only after the removal of the fault that the stabilizing circuits are called into operation. At this time the amplitude of the voltage oscillations is much less than 0.5 p.u. and the system can be considered linear. Consequently, a linear model of the system can be considered appropriate and in the present study the system response for a pulse of B equal to 100 p.u. corresponding to reactance of X = 0.01 p.u. was retained for the identification of the system

3.3   System Identification for the observable modes at the control bus

Spectrum analysis was carried out on the output voltage and frequency to obtain the major frequency components present in the waveform. These were .068, .88, 1.25 Hz as also shown in the figure 3.4.
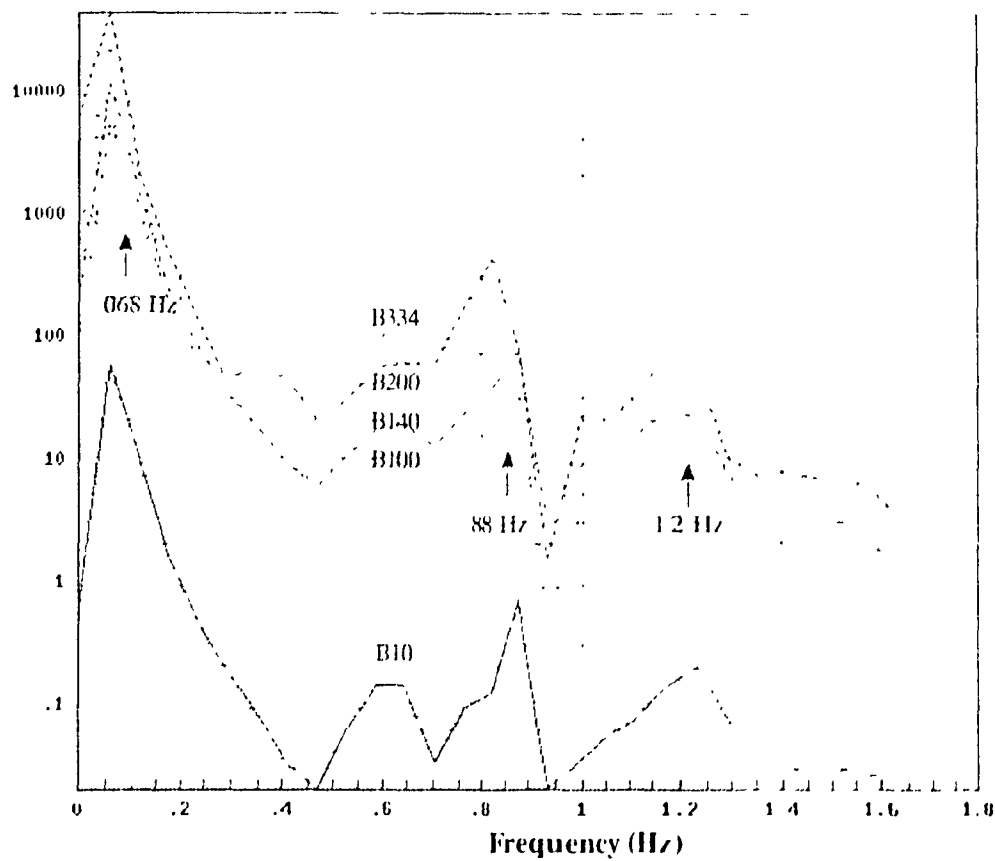

Figure 3.4 Power spectrum of output frequencies for different pulses

In the process of system identification a set of transfer function blocks are built with the curve fitting technique to obtain the same response in terms of voltage and frequency from these blocks when subjected to the same pulse of B as in the

system. These transfer function blocks have been built with the help of Matrixx, a general purpose mathematical software package. The blocks used are second order functions, in which adjustment of damping was carried out to match the system response.

A second order function can be represented as

$$C(s) = \frac{k\omega_n^2}{s^2 + 2\zeta\omega_n s + \omega_n^2}$$

(3.4)

where ω_n is the natural frequency of oscillation and sigma is damping factor.

In the time domain the output of a underdamped second order function to any impulse input is oscillatory initially and then settles down to its original state in a manner dependent upon the damping(provided the damping factor is greater than zero) and natural frequency of the function. The transfer function of the system is built up with the help of parallel combinations of many second order blocks representing the different modes of oscillations defined by the spectrum analysis of the simulated results.

The addition of the output of these gives the change in frequency as observed at that particular bus for a given change in the susceptance input. The voltage signal is also obtained from the same set of blocks with some corrections applied to phase and gain of the signal. The connection of the set of blocks is as shown in the figure 3.5 where each individual block represents a first or second order function as defined by the equation 3.4.

The transfer function for these blocks as shown in the figure 3.5 are given in the appendix A There are five sets of transfer function blocks used (one blocks is of first order and four are of second order). The input B is given to all these blocks simultaneously and output is summed up to recreate the signal which is similar to frequency deviation as obtained from the stability program. The output of each block

is further treated to formulate the signal corresponding to voltage output signal. The value of B used for simulation in the simulation (matrix) and in the stability program was 100 p.u.
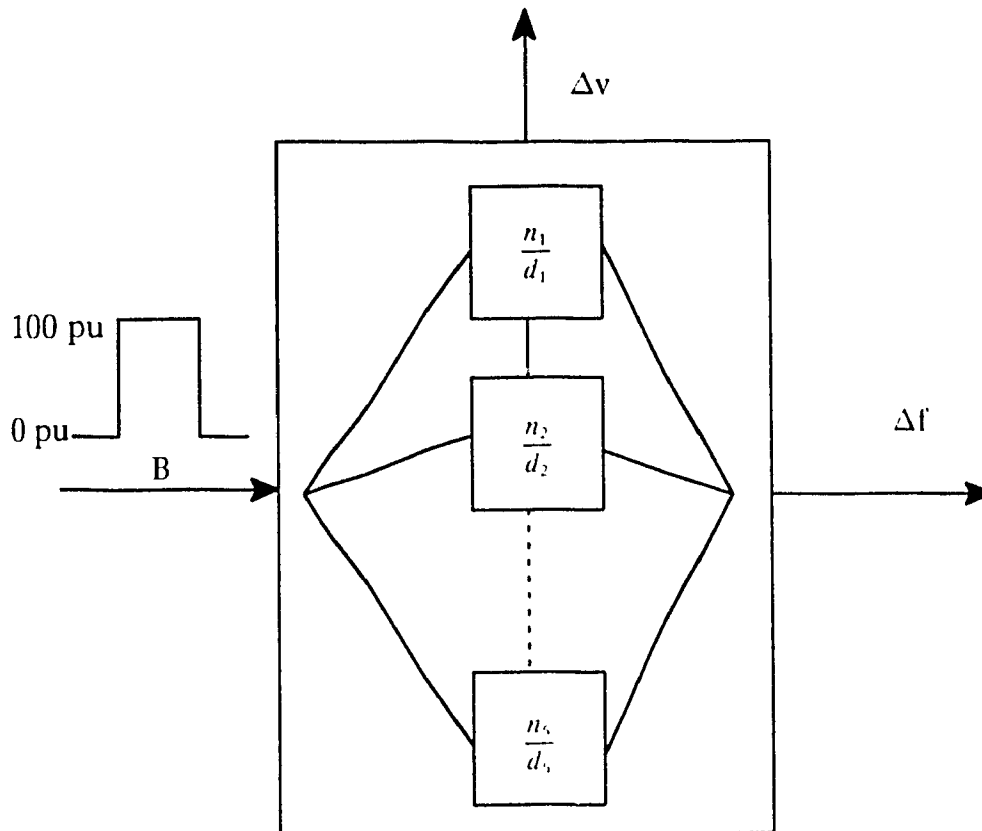
Figure 3.5 Power system transfer function representation in matrix

The total transfer function so obtained gives the relationship between change in susceptance B at that particular bus and the resulting changes in voltage and frequency.

Figures 3.6 and 3.7 show the frequency and voltages responses of the set transfer function blocks superimposed on the responses obtained from the time domain simulation of the detailed system for the same input.

Figure 3.6 Output frequency deviation from simulation (detailed) and matrix model

Figure 3.7 Output voltage deviation from simulation (detailed) and matrix model

The close proximity of these curves indicate that the system as identified by
the reduced order transfer function can be taken as an equivalent of the detailed
system for changes in the linear region.

3.4   SVC Modeling

To the system model as identified above a SVC with only voltage
control loop is added in the simulation study and also in the matrix model. The SVC
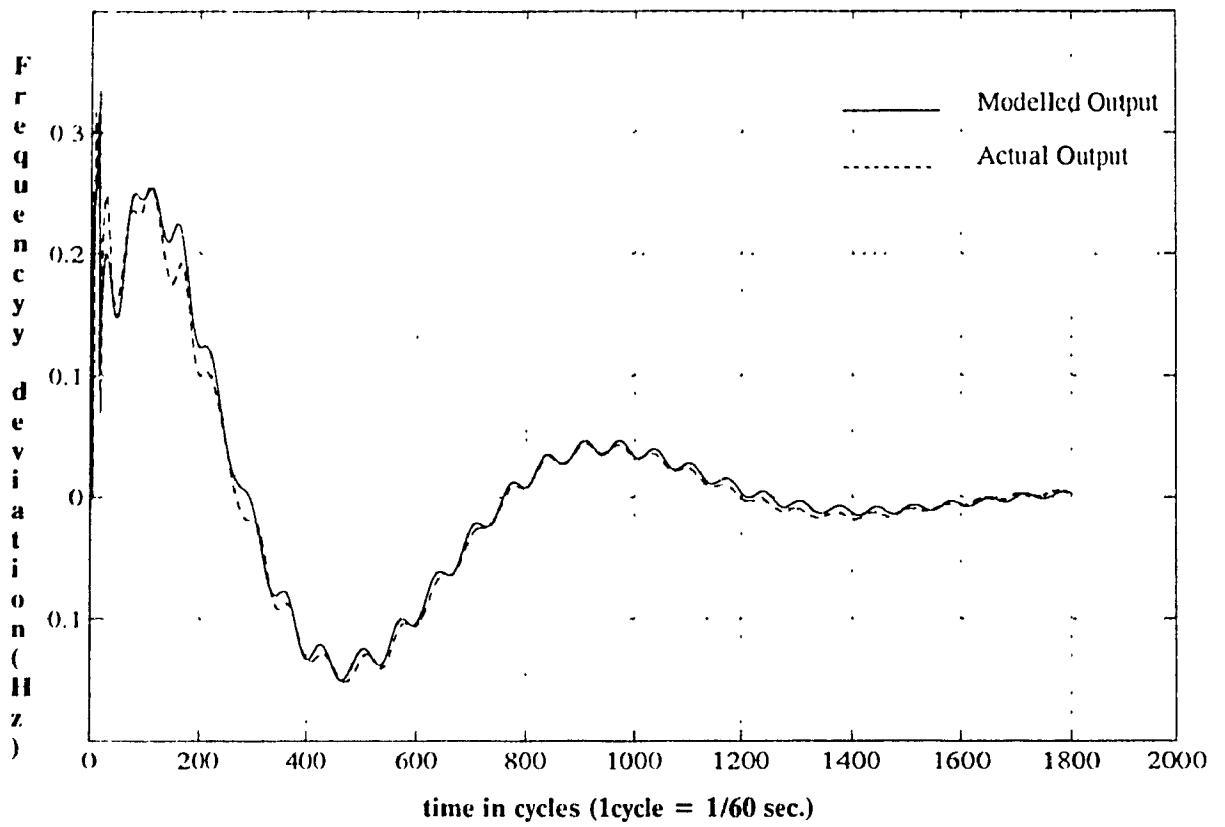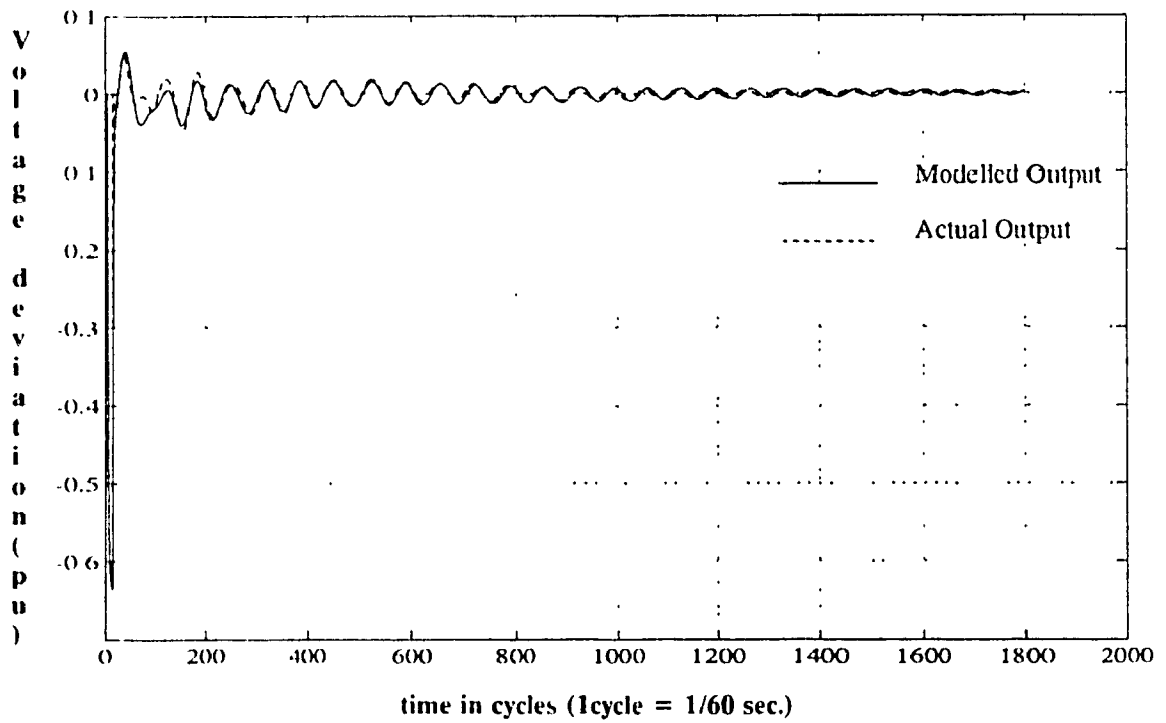model used for this study (as represented in the Load flow and stability program)
is composed of mainly two units thyristor controlled reactor (TCR) and thyristor
switched capacitor (TSC). The basic structure and the modelling details are discussed
in the following section.

Thyristor controlled reactor is basically a reactor of fixed inductance L
in series with a pair of thyristor valves connected in reverse-parallel for bidirectional
conduction. The current in the reactor is controlled by changing the firing angle of
the thyristors. The current and the duration of conduction is maximum for $\alpha = 90$
when either one of the thyristors conducts all the time. As the firing angle is increased
from 90° to its maximum value of 180° the conduction interval and the effective value
of the current flowing through the thyristors reduces, which is equivalent to a change
in the reactor inductance and thereby a change in the reactive power.

Thyristor switched capacitor consists of capacitors connected to a pair of
thyristors connected for bidirectional conduction with a small inductor in series to
limit the current peaks during capacitor switching. Typical representations for TCR
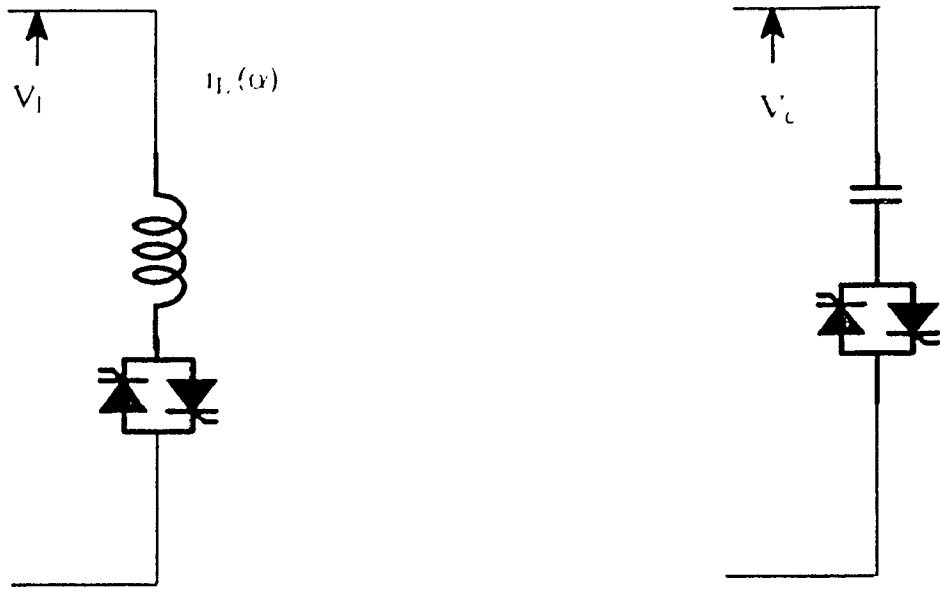and TSC are as shown in figure 3.8

Figure 3.8 Representation of TCR and TSC

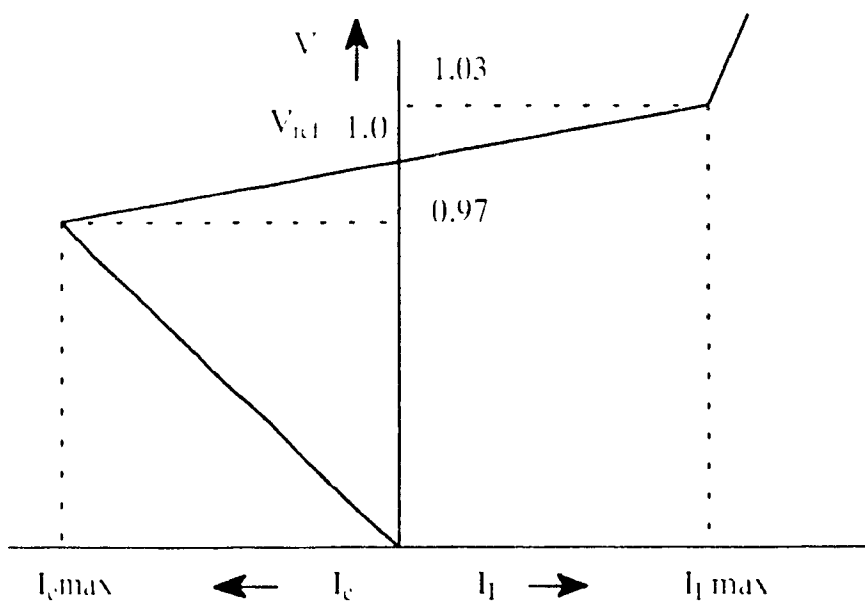The VI characteristic of the TCR+TSC type SVC is as shown in figure(3.9)

Figure 3.9 VI characteristic of TCR + TSC

42

As indicated earlier, the SVC under steady state condition is floating on the bus, that is, its output is practically zero and it is neither inductive nor capacitive. This voltage is termed as reference voltage (V_{ref}) and is obtained from load flow program. If the system voltage changes because of any disturbance, the SVC control block will compare the new voltage (V_t) at its terminals with V_{ref} and an error signal is fed to the regulator to determine the value of susceptance B (capacitance or inductance). The value of desired susceptance B is converted to a signal which controls the firing angle of the thyristor valve and switching of reactive or capacitive branches. The value of desired susceptance B is proportional to reactive power needed by the system to correct its voltage to the desired (V_{ref}) value.

In practice the terminal voltage is allowed to be different from its reference value V_{ref} by a value determined by the droop characteristics as shown in figure 3.9. The value chosen for this study is a droop of 3% which means that the terminal voltage is allowed to vary between 0.97p.u. (considering reference voltage of 1p.u.) for SVC being fully capacitive and 1.03p.u. for SVC being fully inductive. The droop characteristic of an SVC is necessary to ensure the stability of the SVC. Having no droop (that is droop = 0%) might result in multiple operating points with the SVC oscillating between inductive and capacitive regions. If the voltage rises above or falls below the predetermined levels as defined by the droop characteristics (1.03 p.u and 0.97 p.u.) for our case, the SVC behaves like pure capacitor or inductor and the var output is proportional to applied voltage and the fixed susceptance.

The block diagram of the SVC used for this study is shown in the figure 3.10. It basically consists of the following blocks
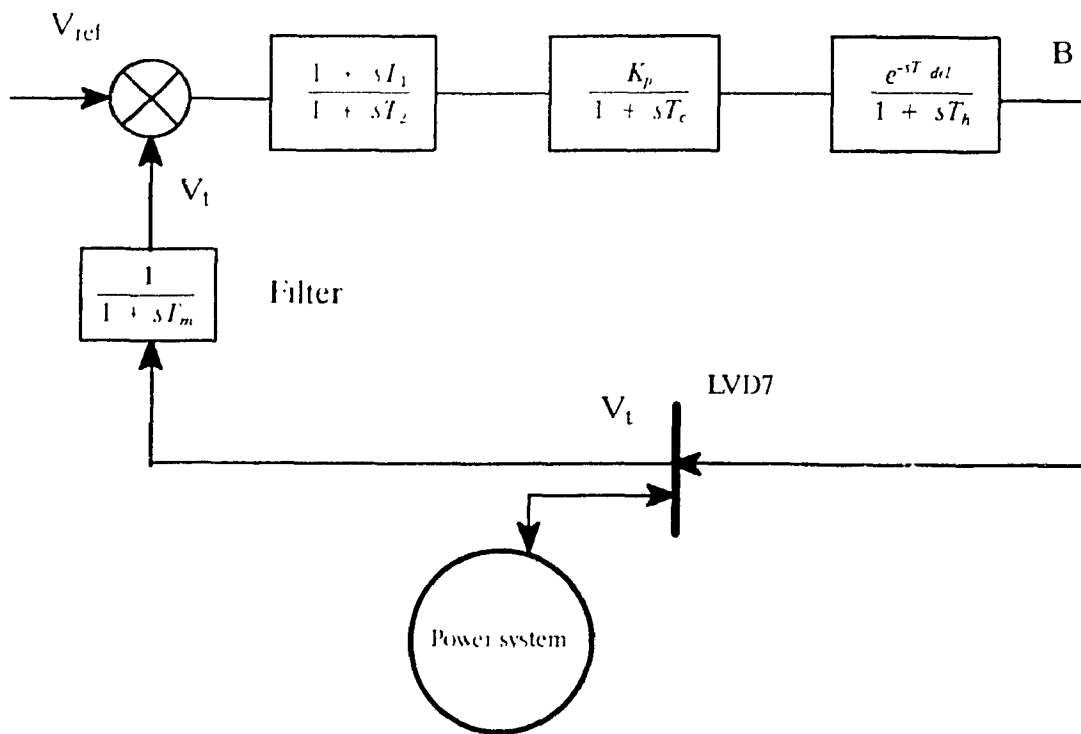
Figure 3.10 Block diagram representation of SVC and connected network.

- voltage measuring and filter circuit which is represented by a a single order lag circuit $1/(1 + sT_m)$ where T_m represents the measuring and filter time constant

- Voltage regulator control block representing the lead-lag compensation circuit.

- Gain Kp to represent droop characteristics of the voltage and an integral controller.

- Thyristor action is represented by $(e^{-s}{}_{del}) / (1 + sT_{th})$ where I_{del} is the gating transport delay and T_{th} represents the additional time constant representing the effect of thyristor firing sequence control.

3.5   Validation of Identified Transfer Function with addition of SVC

This model of the SVC is introduced in the transfer function model defined in the matrix environment. A pulse of B is applied to the system and analysis is carried out for a time period of 30 seconds(1800 cycles). The response is compared to the output as obtained from the stability program and the two are superimposed as shown in figure(3.12)
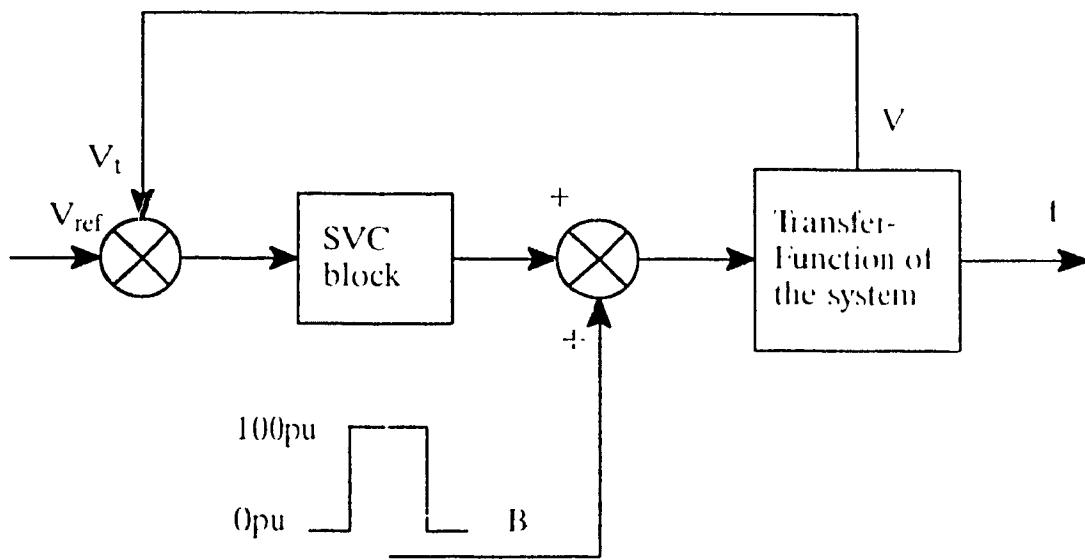
Figure 3.11   Block diagram representing
addition of SVC to transfer function block

V_t is the measured terminal voltage and V_{ref} is the pre disturbance terminal voltage.
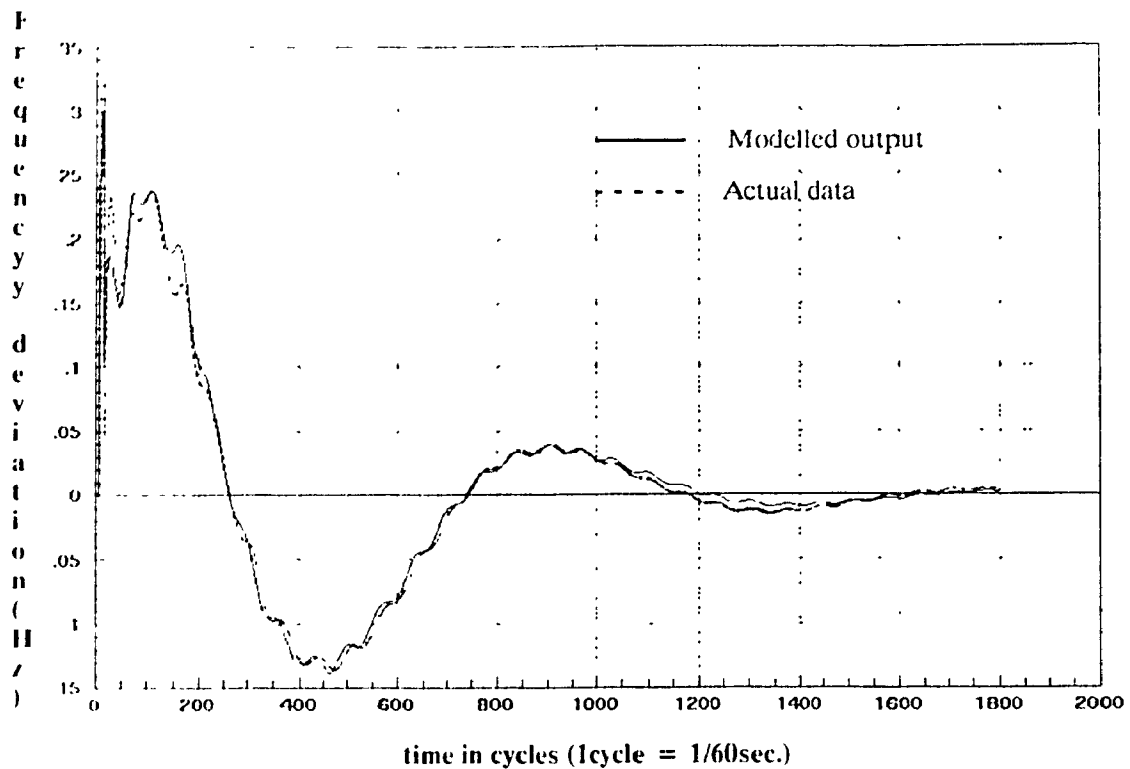
Figure 3.12 Output Frequency at LVD7 with SVC model

The output frequencies in the two cases match close enough to validate the identified transfer function model and the addition of SVC block.

3.6 INTER MACHINE OSCILLATIONS NOT OBSERVABLE IN THE FREQUENCY

The system transfer function identified above gives the set of blocks which define the relationship between change in susceptance B and the resulting change in voltage and frequency at the same bus This model has been used to design a controller to damp the load mode (0.68Hz) and the two swing modes (0.88 and 1.25 Hz) which

could be observed in the frequency signal. In addition to the above there is another swing mode (0.55 Hz) between 1 G and CHU which could not be observed in the frequency signal. To facilitate the design of a separate loop to damp this mode a second system identification block was determined.

The figure 3.123 shows the response of the angle difference for changes in B at LVD7 bus and figure 3.14 show its frequency spectrum.

time in cycles (1cycle = 1/60sec.)
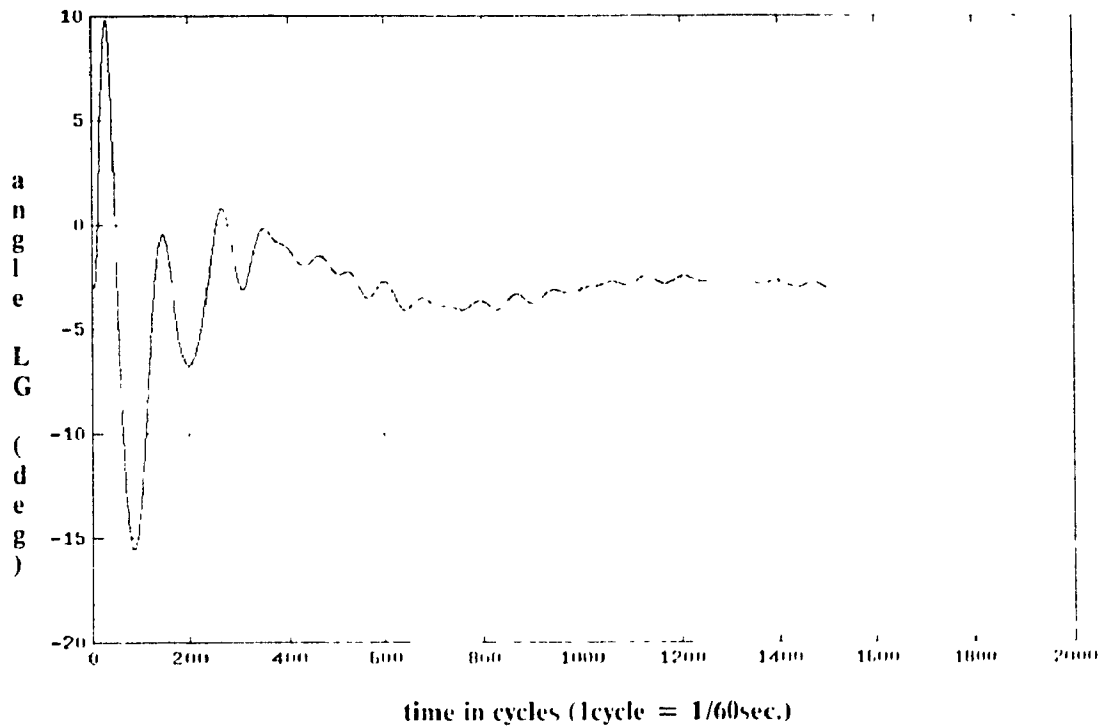
Figure 3.13 Angle between machines at 1G and CHU
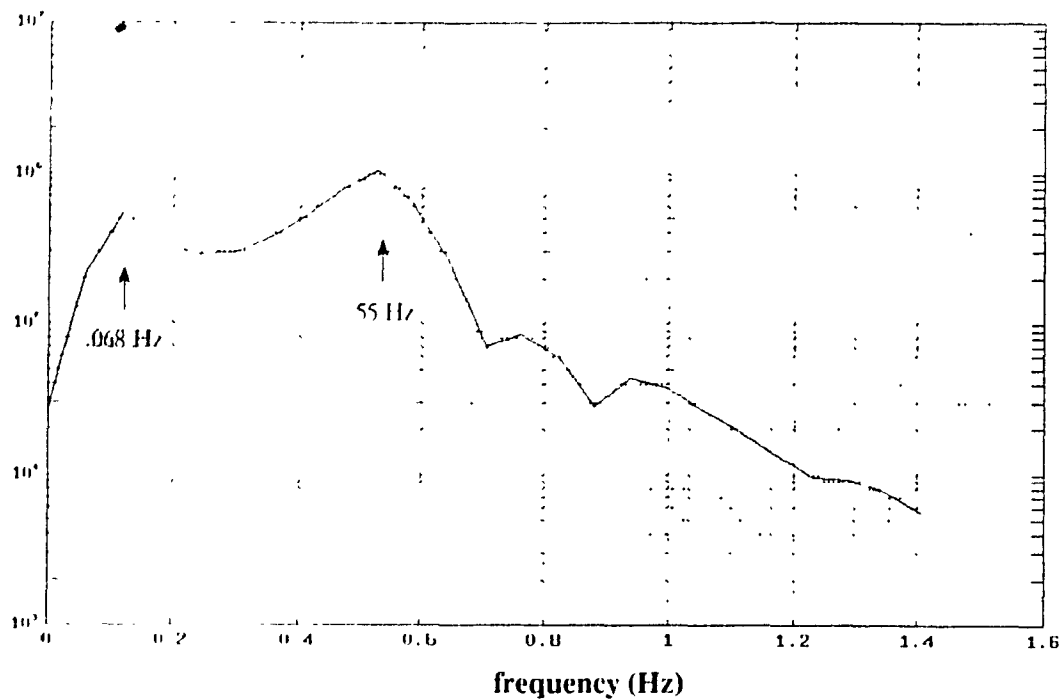
Figure 3.14   FFT analysis on the angle difference between LG and CHU

The FFT analysis of the signal corresponding to the angle difference between LG and CHU highlights modes quite different from the modes found by doing FFT on the output frequency. The major frequency in this type of oscillations is 0.55 Hz (this was not observed in the FFT analysis of the frequency at the control bus LVD7) and a low frequency component varying from 0.068 to 0.1 Hz.

A transfer function block was identified to model the relationship between the angular difference and B. The response of this transfer function is compared to that obtained by simulation, in figure 3.16. The figure shows that the system is well identified for one of the intermachine oscillations not observable in the frequency signal at LVD7 bus.
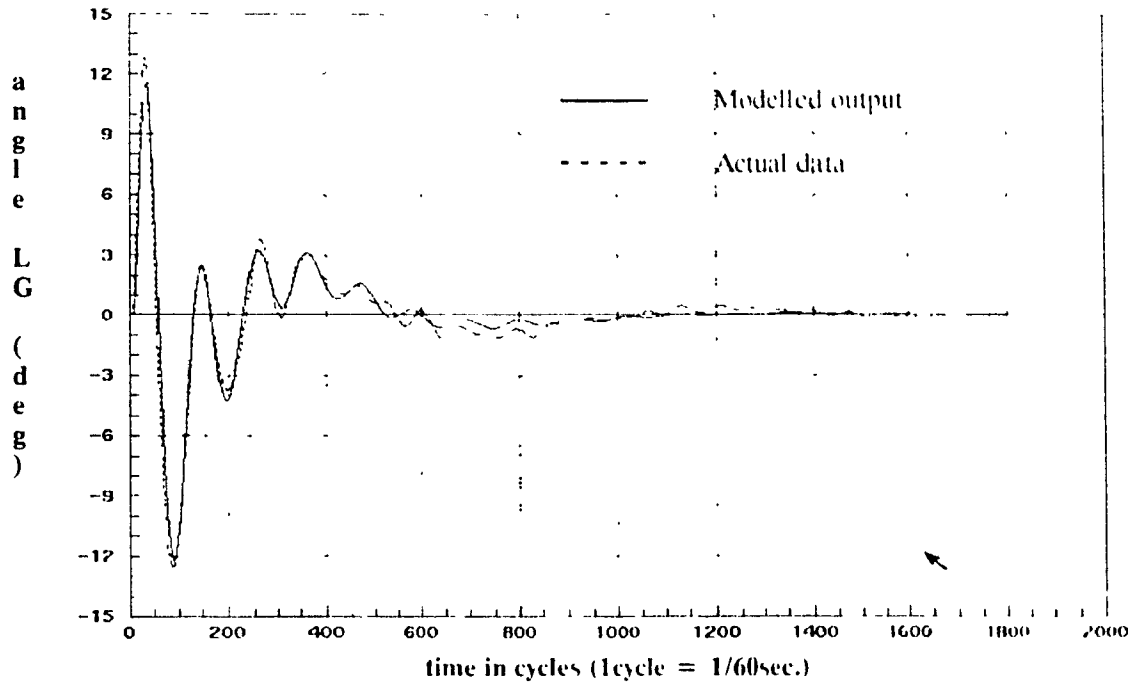
Figure 3.15 Machine angle at LG3 (ref CHU) simulated/reduced model

The complete system is now defined in terms of two transfer function for the same input pulse of B and different outputs as shown in the figure 3.16
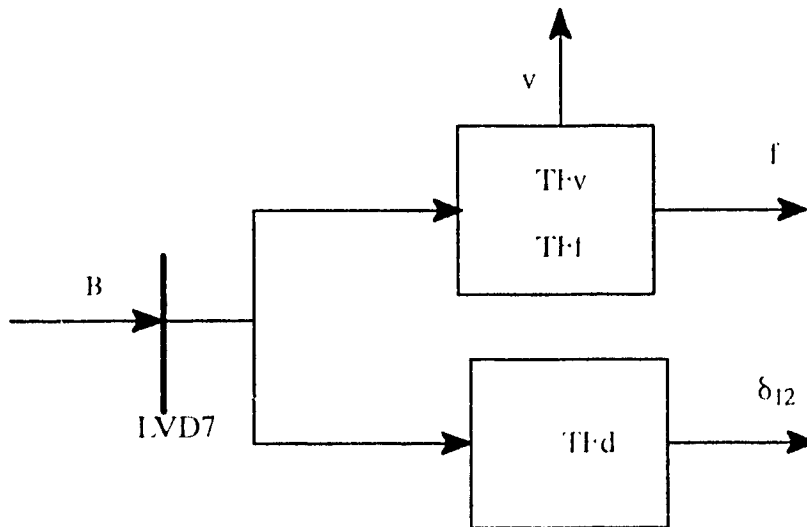
Figure 3.16 Block diagram representation of the two transfer functions.

In the first transfer function block the part Tfv is necessary to complete SVC voltage control loop. Blocks Tlf and Tld are necessary for the regulator to damp out the load mode and swing mode oscillations.

The design of these controllers is the subject of the next chapter.

Chapter 4

Design of Feedback Controllers

4.1   Introduction

It was mentioned in chapter 2 that two modes of oscillation (inter machine and load modes) can exist in a system and whereas it is obvious that load mode can be controlled by modulating the load, it was shown that the swing mode (between machines) can also be controlled by the load modulation. It was also shown in chapter 2 that of the three location of SVC's on the system the maximum voltage variation and hence the load variation, is obtained by controlling the reactive power at the LVD7 bus.

In the present chapter, the design procedure for supplementary loops in the SVC at LVD7 will be described. In the first controller, the frequency at the LVD7 was taken as the controlled variable. The design and performance of a second supplementary loop for damping the swing mode oscillation between LG and CHU

is also discussed. The affect of introducing the supplementary loop is examined and its parameters optimized. The well known root locus technique was used to study the affect of different parameters on the damping of the different modes.

4.2   Open Loop poles

Table 4.1 gives the open loop poles of the system including the SVC with its voltage control loop. These poles are plotted in the S plane and shown in the figure 4.1. These poles correspond to the transfer function which relates susceptance B and frequency f. The fact that all the roots are on the left half of the S plane shows that the system is stable but as also seen from the plot, the roots of frequencies of interest (this corresponds to item 2, 6 and 7 in the table 4.1 and figure 4.1 which represent the low frequency of interest that are 0.0683 Hz, 0.88 Hz and 1.2 Hz respectively) are located very close to the Y axis indicating very little damping at these modes. The objective of the supplementary loop will be to increase the damping by moving these roots more to the left in the S plane.

S. no.	pole
1.	$-0.245 \pm j0.000$
2.	$-0.179 \pm j0.3998$
3.	$-0.800 \pm j0.000$
4.	$-4.720 \pm j0.000$
5.	$-3.620 \pm j3.1113$
6.	$-0.148 \pm j5.5664$
7.	$-0.8242 \pm j7.8358$
8.	$-14.044 \pm j7.2760$
9.	$-49.962 \pm j0.00$
10.	$-125.0 \pm j0.00$

Table 4.1   Open loop poles
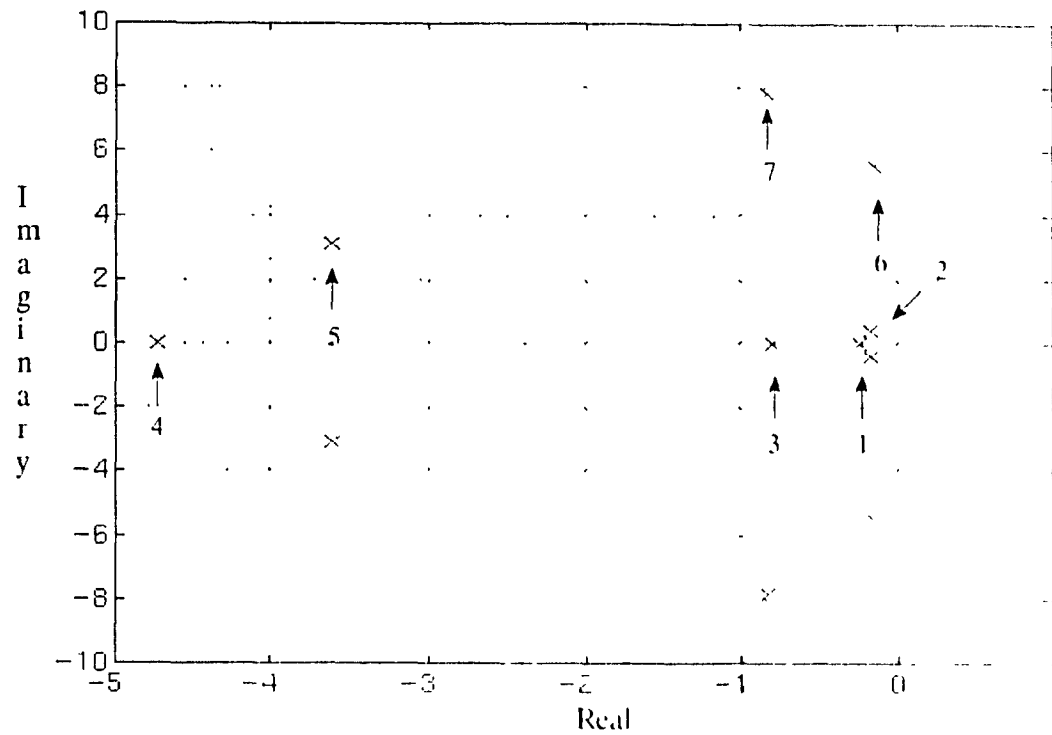
Figure 4.1 Open loop poles

4.3   Design of Feedback Controller with Frequency Signal as Feedback

The figure 4.2 represents in block-diagram form the system with its feedback circuit. The block G(s) represents the transfer function of the system as viewed at the bus LVD giving the variations in the frequency for changes in suscep tance B at the bus and the feedback loop H(s) represents the SVC supplementary loop Also as shown in the figure 4.2 the output variable (or input variable to the feedback block H(s)) is frequency but it can be any other variable like the intermachine swing between two machines which seems to be critical (near instability) and requires addi tional damping.

The output from the supplementary block is fed into the summing junction of the SVC. Thus the final susceptance B produced by the SVC will have a component that is dependant on frequency or the other variable.
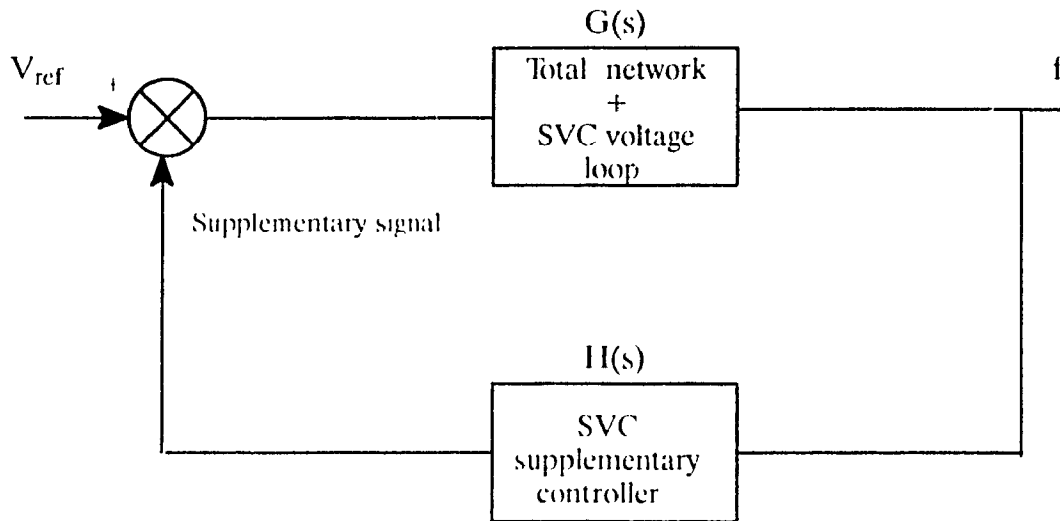
Figure 4.2 System with supplementary feedback loop

The transfer function of the closed loop system shown in figure 4.2 is

$$= \frac{G(s)}{1 + G(s) H(s)} \qquad (4.1)$$

The denominator of the equation (4.1), that is, 1+G(s)H(s), represents the characteristic equation of the system. In the root locus technique the roots of the characteristic equation also named as eigenvalues of the system, are plotted (in the S plane) with the variation of gain k in the feedback circuit. The necessary condition for the stability of the system is that all the roots of the characteristic equation or the eigenvalues of the closed loop system must be located in the left half of the S plane.

Initially, to evaluate the effect of adding a frequency dependant signal as feedback, the loop was closed with the feedback loop H(s) simply representing a block of pure gain (k). The root locus plots for the system are shown in the figure 4.3 for variation of gain.
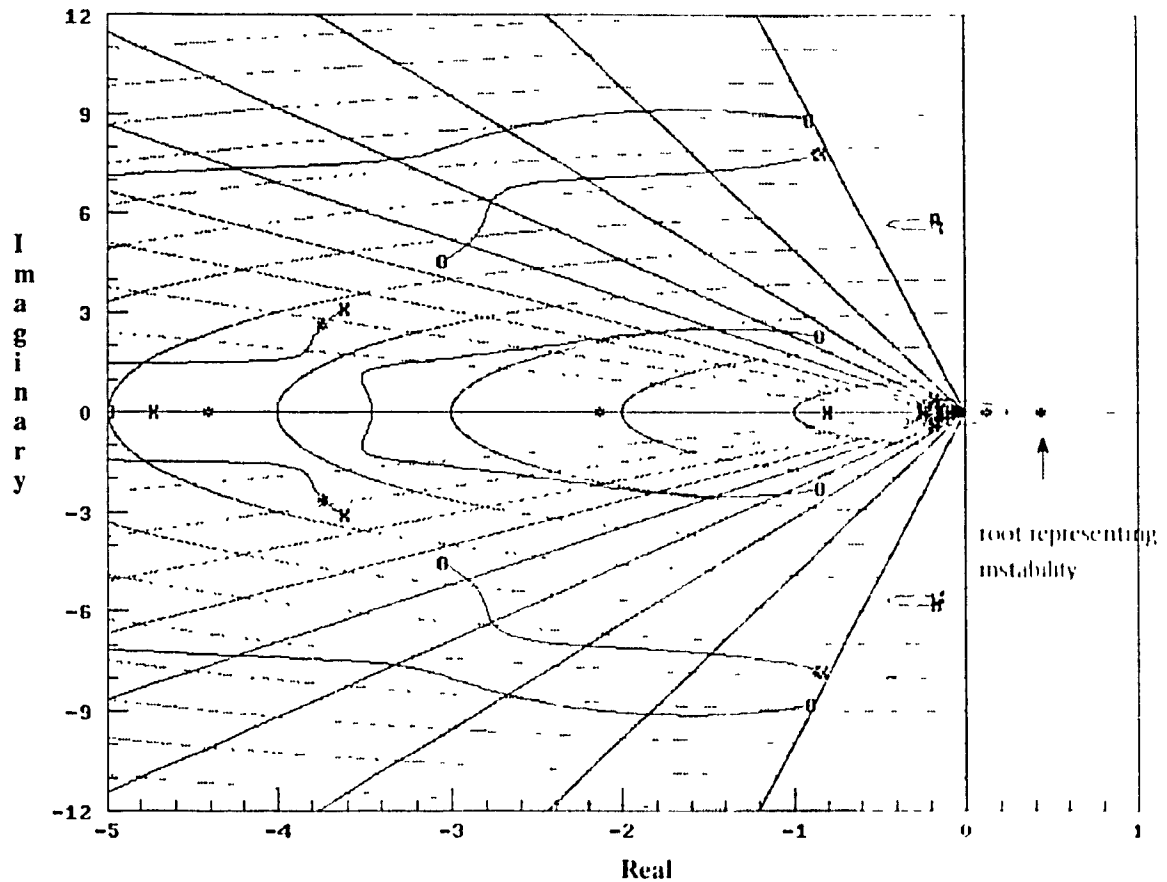
Figure 4.3   Root locus with frequency(with gain k) as feedback signal

Two points were observed from this plot : firstly that even with small variations of gain k the roots corresponding to the slow frequency component (f 0.0683 Hz) were crossing over to the right side indicating instability for this mode with the closure of the loop. Secondly, for the roots corresponding to the other major frequency components of interest (0.88 Hz and 1.2 Hz) there is only a small movement to the left. This implied that the feedback loop gain must have a block that is a function of frequency, having low gain at low frequencies and high gain at high frequencies.

One way of doing this is to add a block in the feedback circuit, usually referred to as a washout block, having the form $\dfrac{sT}{1+sT}$. In this study T_1 was chosen as 2.75 seconds.

The gain of this block as a function of frequency is shown in figure 4.4. It behaves basically as a high pass filter introducing a fractional gain (negative in dbs) at low frequencies and approaching 1 (0 db) as frequency increases.
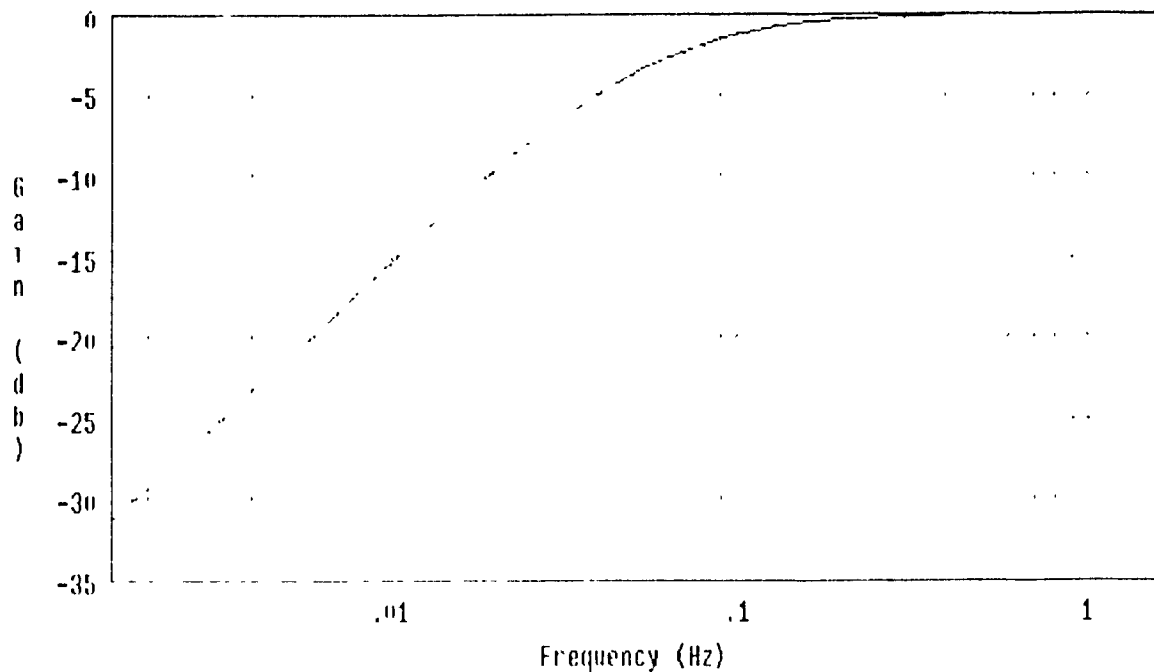
Figure 4.4   Bode plot for washout block (High Pass Filter)

With this block it was found that it was possible to move the higher frequencies roots slightly to the left in the S plane without the 0.0683 component going unstable However the improvement was limited and as the gain was increased the lower frequency became unstable It was then decided to introduce an additional second order filter for further reducing the gain on this particular frequency. The transfer function of this filter is of the form $\dfrac{A}{B+\ldots}$ This filter introduces a further re-

duction in gain about -30 db for 0.0683 Hz while for frequencies 0.5 Hz and above the gain is 0 db, that is the original signal goes through without any modification. The bode plot for this filter is shown in the figure 4.5.
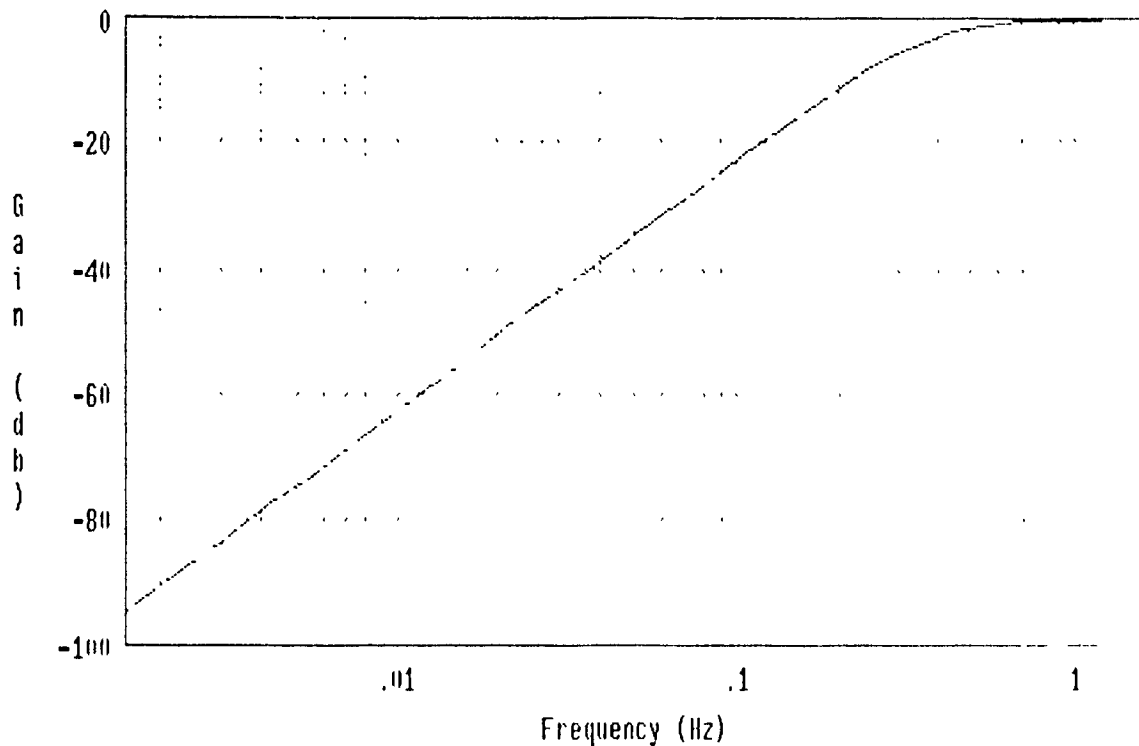
Figure 4.5 Bode plot for second order filter (High Pass Filter)

To the blocks described above, lead/lag compensator and the limiter blocks were added. The lead/lag blocks are necessary to correct the phase and gain of the different frequencies in the feedback signal. The limiter block is added so that the output of SVC (with its voltage control loop) is not affected by a large magnitude under transient conditions but it is still able to damp out the oscillations. The limits of the limiter block were fixed at 0.1 (maximum) to 0.1 (minimum). The final structure of the supplementary block is shown in the figure 4.6

Wash out Filter Gain

Δf

$$\frac{s T_1}{1 + s T_1}$$

$$\frac{k s^2}{s^2 + B s + \omega_n^2}$$

$$k$$

Lead / Lag
Compensator

0.1

SVC summing
block

limiter

V_{ref}

$$\frac{1 + s T_2}{1 + s T_3}$$

$$\frac{1 + s T_4}{1 + s T}$$

V_s

V_t

−0.1
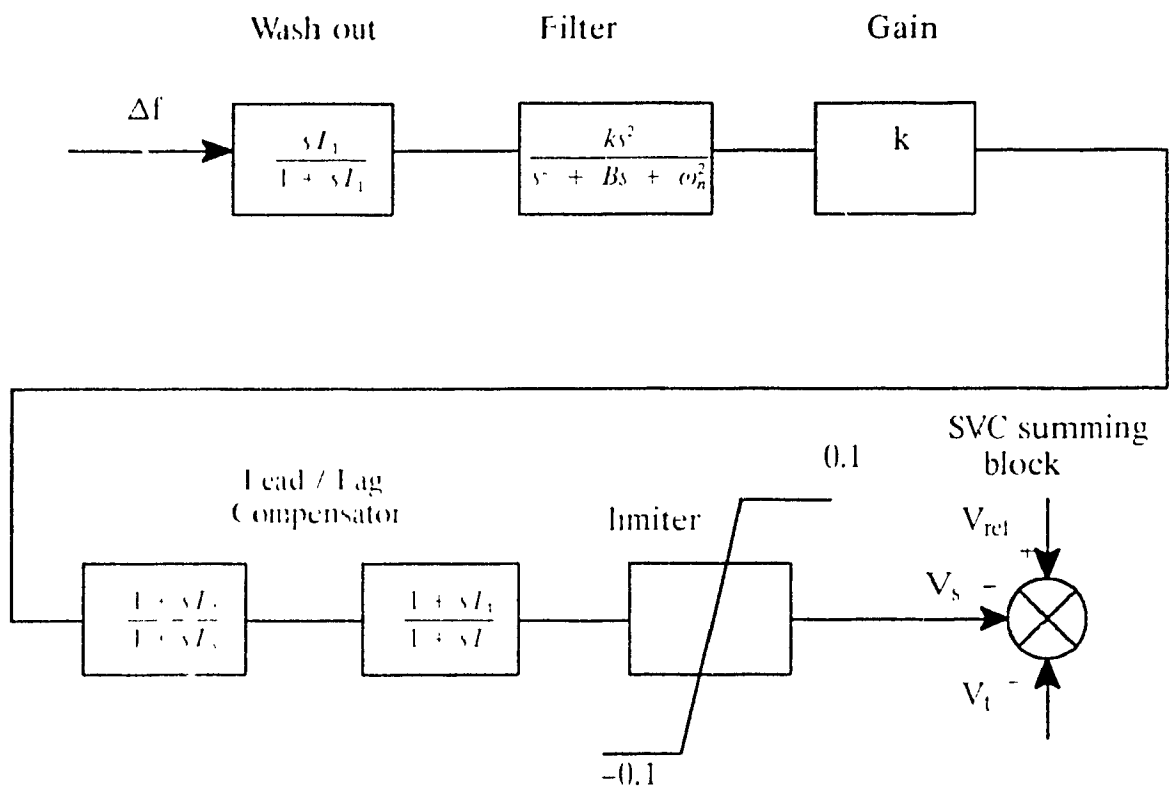
Figure 4.6 SVC supplementary loop

These set of blocks as shown in the figure 4.6 form the function H(s), defined in the figure 4.2. The block G(s) (refer figure 4.2) is the transfer function of the network with its voltage control loop. Based on the various plots of root locus the values were finalized for the various time constants that is from T_2 to T_4 for lead lag circuits and also the value of gain k.
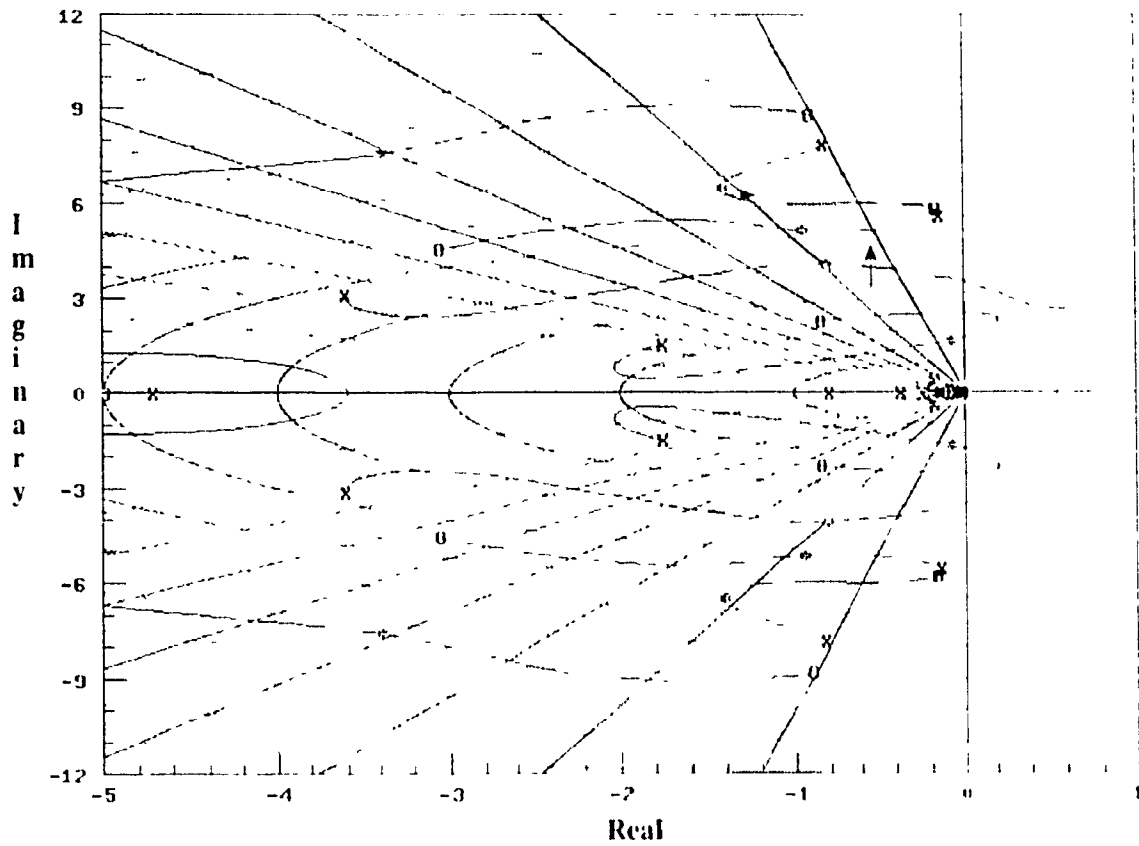
Figure 4.7 Root locus with supplementary loop

The final plot of the root locus plot with the supplementary loop is as shown in the figure 4.7. The lines originating from the origin correspond to the constant damping ratio. Their are ten lines in each half of s plane representing the variation of damping from 0.1 to 1.0 in steps of 0.1. It can be observed from this root locus plot (figure 4.7), that for the roots corresponding to 0.8 Hz and 1.2 Hz the damping increased from 0.027 to 0.2 and from .1 to .2 respectively. The new position of roots of interest is highlighted by arrow marks in figure 4.7. The damping for the pair of roots corresponding to the second order filter was reduced to a value less that 0.1. This is acceptable as the system is not resonant at that particular frequency

4.4　Simulation Results using Matrix Model

　　　　Simulation was carried out in the software package Matrixx described earlier, with the same value of disturbance as used for system identification, to determine the influence of the addition of the supplementary loop. The results of the same are as shown in the figure 4.8 below.

time in cycles (1cycle = 1/60sec.)

Figure 4.8 Output frequency at TVD7 without and with supplementary loop using Matrix model

These results clearly indicate that the supplementary loop has helped increase the damping of 0.068, 0.88 and 1.2 Hz oscillation.

The design parameters have also been tested by time domain simulation using the transient stability program ST600 program and the results are presented in the next chapter.

4.5   Design of Controller for LG – CHU Swing Mode oscillation

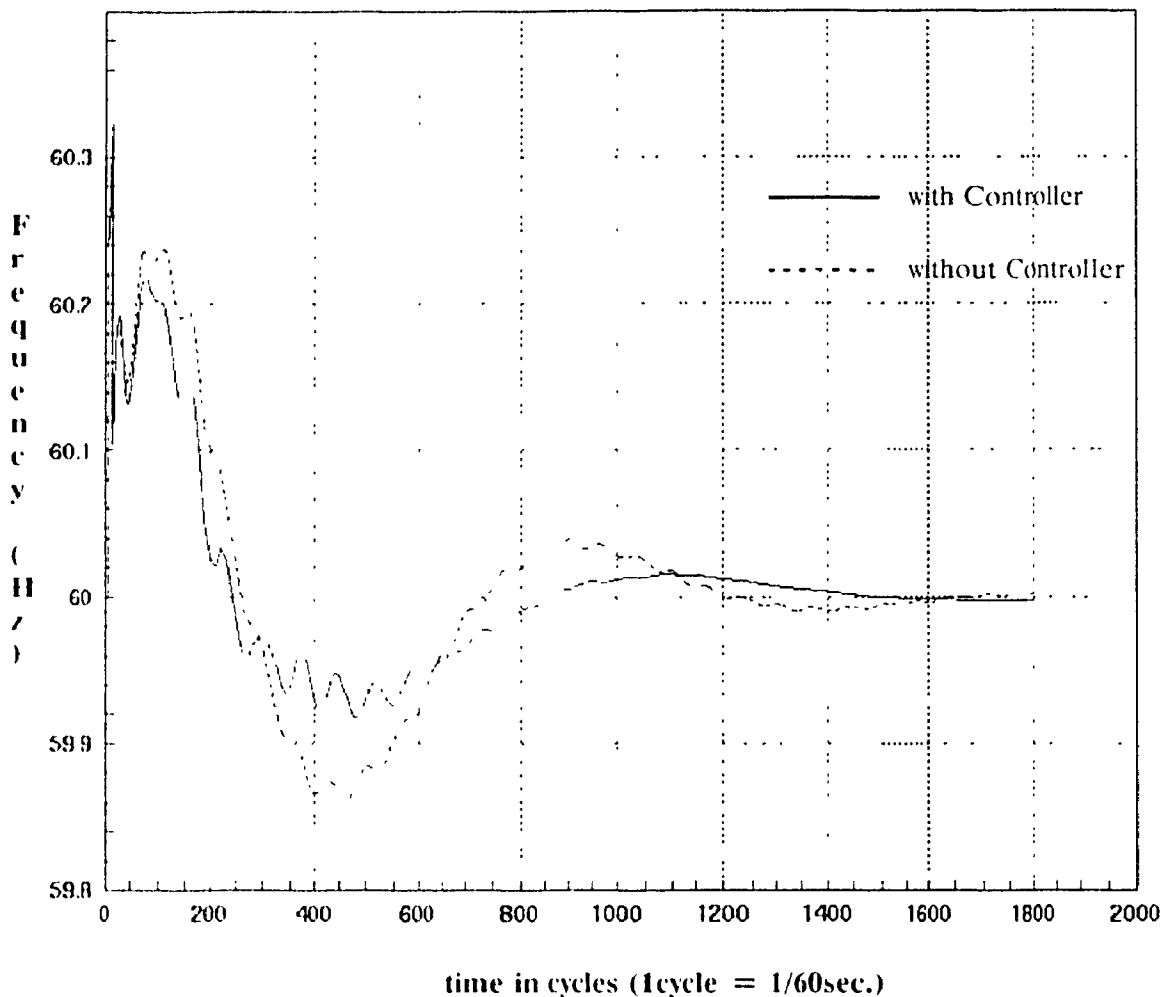The choice of the input variable for controlling this particular swing mode proved to be a difficult process as this mode is not observable in any of the variables present at the control bus. For the purpose of the present study the angular difference between LG and CHU machine was chosen as the control variable. Some practical difficulties in getting this signal are foreseen due to remote communication but for the purpose of establishing the feasibility of the control technique, these are ignored for the moment.

As discussed in chapter 3, a transfer function was built for establishing the relationship between B and the angular separation between LG and CHU. Using this a supplementary controller was designed to damp this mode.

It was noticed that in addition to the swing mode oscillation of 0.55 Hz present in this signal there was a noticeable component of the 0.068 Hz oscillation as also seen in the frequency signal at the SVC bus. As in the case of the frequency control loop this component had to be completely filtered out

Initially, a similar structure for the supplementary controller was proposed for the control of the LG – CHU intermachine oscillation as designed for the modes observable in the frequency. However during optimisation of the various parameters used in the supplementary block it was found necessary to change some of the blocks. e.g. lead/lag function was replaced by only a lead function. 2nd order filter

as used in the earlier controller was replaced by a block of single order high pass filter. The final structure of the supplementary controller is shown in the figure 4.9.

Wash out   Gain

$\Delta \delta$

$$\frac{sT_1}{1 + sT_1}$$ $$\frac{sT_2}{1 + sT_2}$$ $$k$$

Lead
Compensator   0.1
                    limiter V_{ref}
                                                    SVC summing
$$\frac{1 + sT_3}{1 + sT_4}$$ V_s +   block

                    -0.1 V_t -
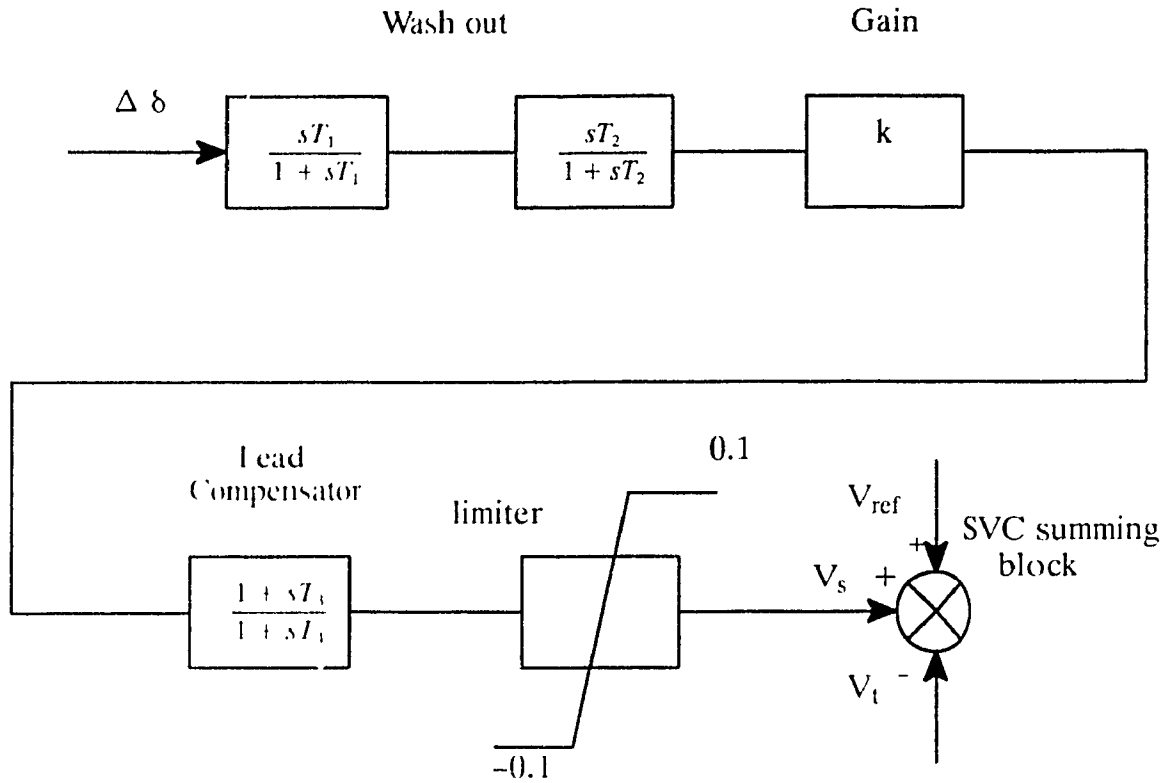
Figure 4.9 SVC supplementary block for angle (LG-CHU) control.

Furthermore, the controllability of this swing mode (LG-CHU) with SVC control is limited and high gain had to be used which made the presence of 0.0683 Hz component in the feedback even more oscillatory if proper filtering was not done.

4.6   Simulation Results with LG – CHU Angle Difference as Feedback

Figure 4.10 shows the response of the system to a pulse of B at the control bus in terms of the angular separation between LG and CHU machines. The continuous line is without the supplementary loop and the dotted line is with it. No appre-

ciable damping is noticeable. This was achieved with an SVC rating of 319 Mvar, the same that was used to damp the modes observable in the frequency.
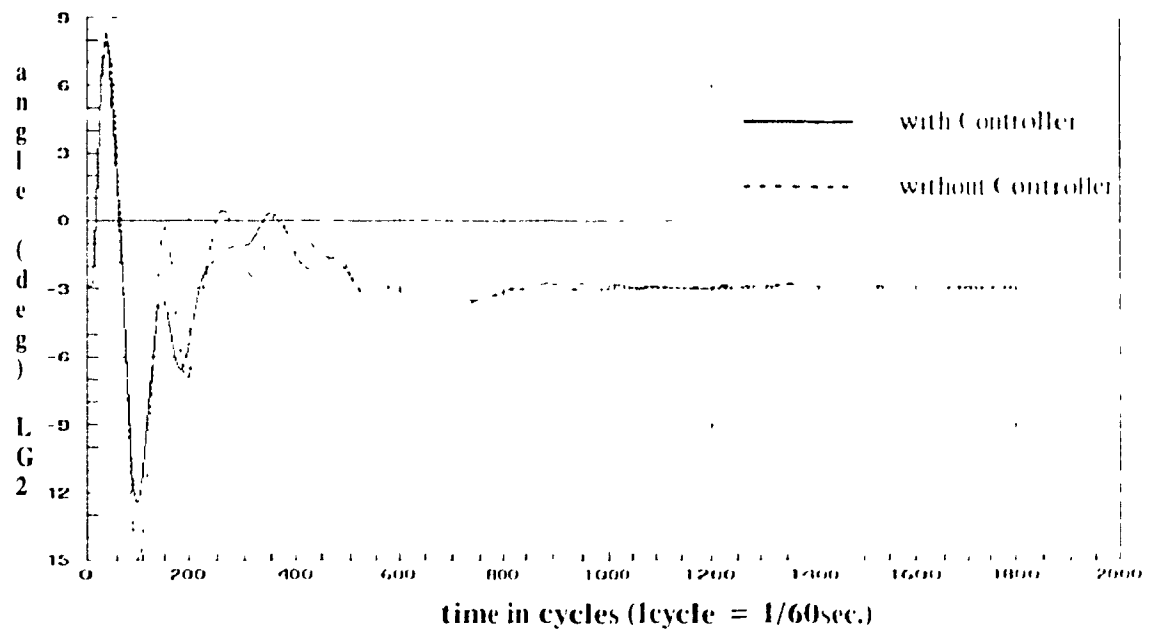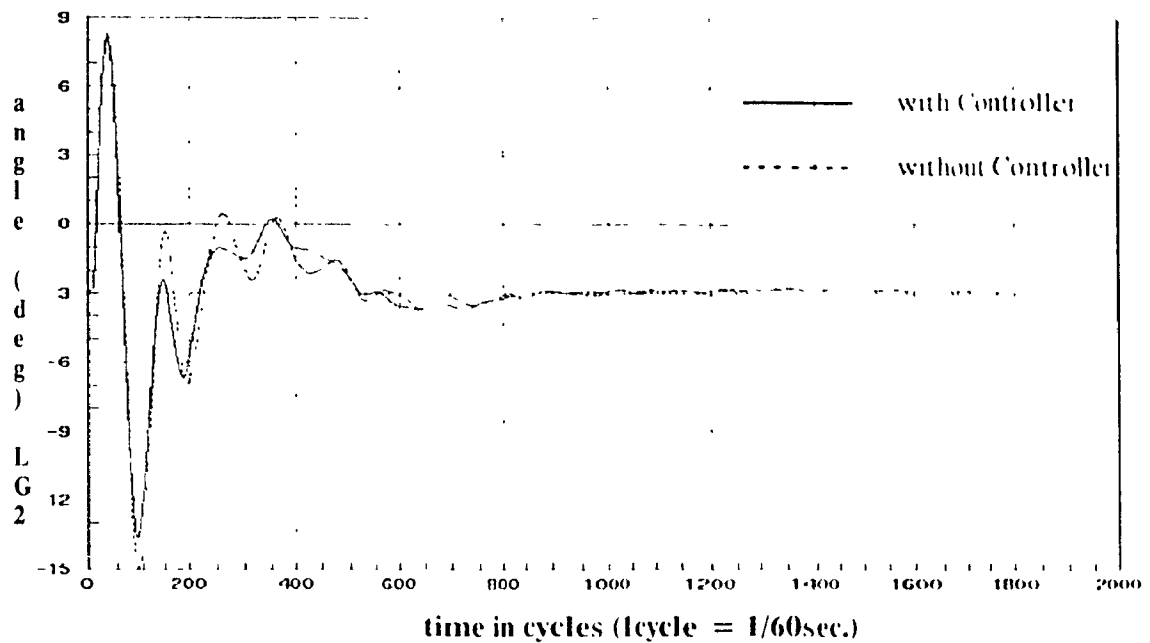
Figure 4.10 Machine angles LG-CHU for different rating of SVC (using Matrix model)

a : 319 MVA

b : 638 MVA

Figures 4.10b show the response under same conditions except for SVC rating which is increased to 638 Mvar. It is seen th t the damping of the swing mode (LG-CHU) can be increased with a higher rating of SVC.

The values of the various parameters were found, using the simulation results on the reduced order model. The parameters of the feedback loop were programmed and interfaced to stability program ST600 and the results are presented in the next chapter.

CHAPTER 5

SIMULATION RESULTS

5.1   RESULTS

The effectiveness of the two separate supplementary controllers was demonstrated in the previous chapter using the reduced order model built in the Matrixx environment. The above design procedure was then verified on the full network using Hydro-Quebec's transient stability program (S1600). A special subroutine representing SVC with its control loop was written and interfaced to stability program (ST600). The listing of this program is given in the appendix B. The controllers were tested individually under same conditions of disturbance and the results are presented in the following two sections.

5.2) Local and Swing modes observable in the frequency

The amount of disturbance for this test case was the same as before that is a pulse of B corresponding to 100 p. u., the plots for frequency at IVD7 are shown in the figure 5.1. Both these curves are with SVC in service however the first curve represented by continuous lines represent the SVC plus controller in service
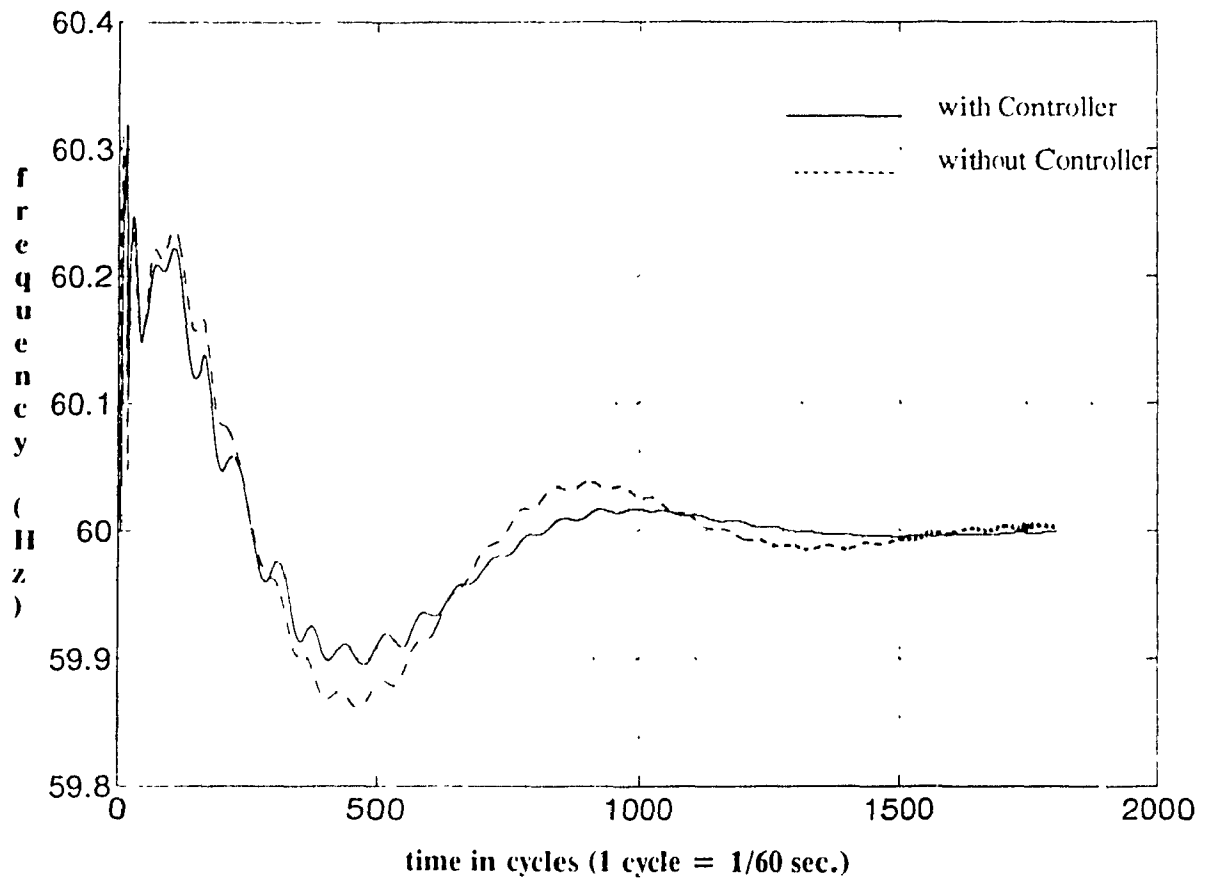
Figure 5.1 Output frequency using stability program at LVD7 (with SVC and with and without supplementary control.

For the conditions described above the following plots compare the machine angles for different machines at the location Le Grande identified as LG and MIC3 (refer to chapter 2, figure 2.6) for two cases, one with just SVC in service and second with SVC plus its supplementary controller.
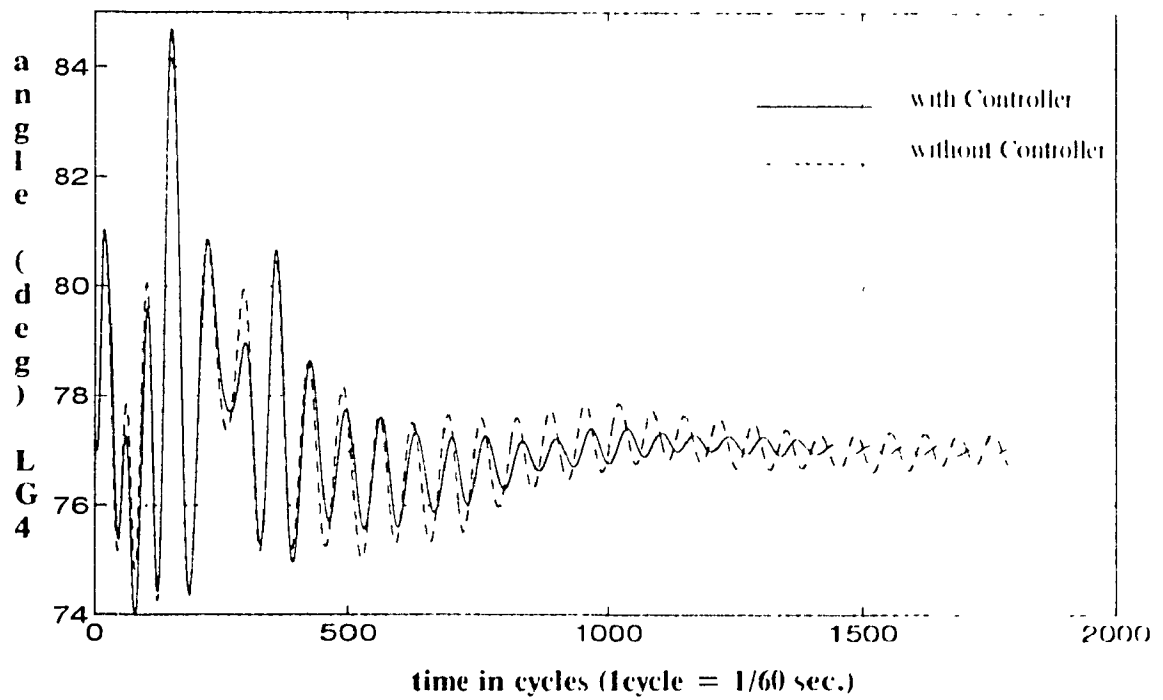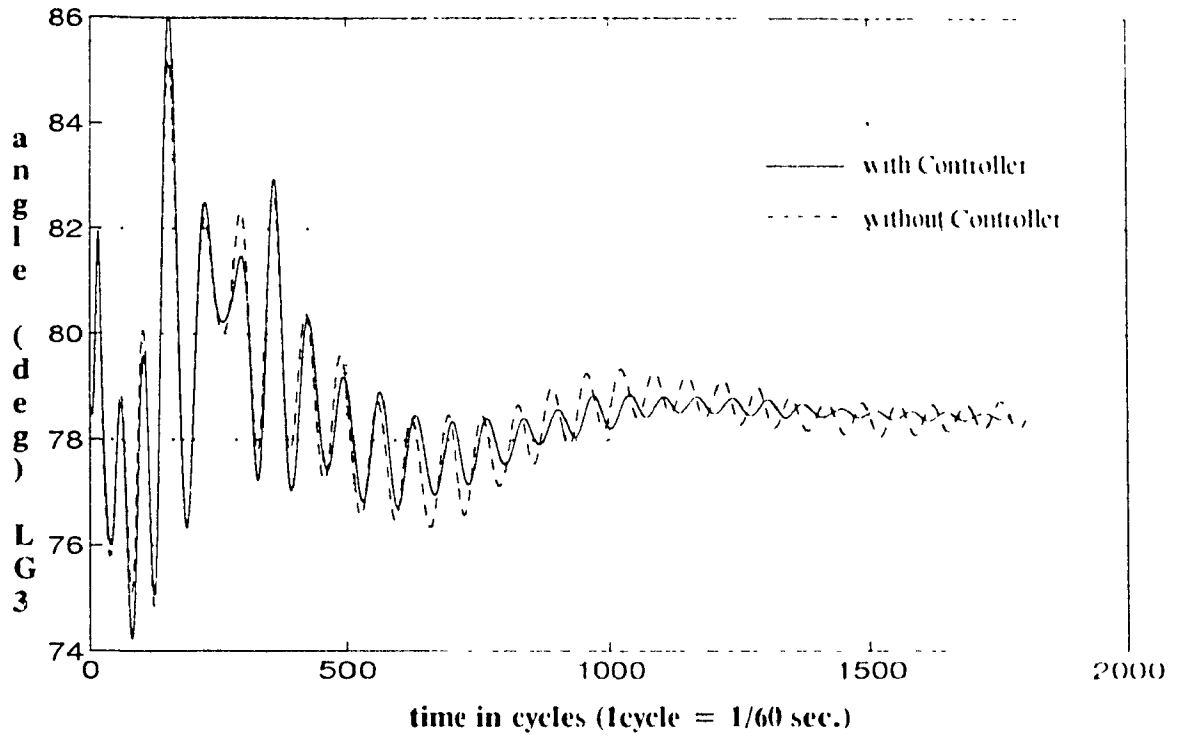
Figure 5.2 Machine angles (with ref. to MAU3) for machines at LG (with SVC plus frequency input supplementary control and with SVC alone)

with Controller

without Controller

time in cycles (1cycle = 1/60 sec.)
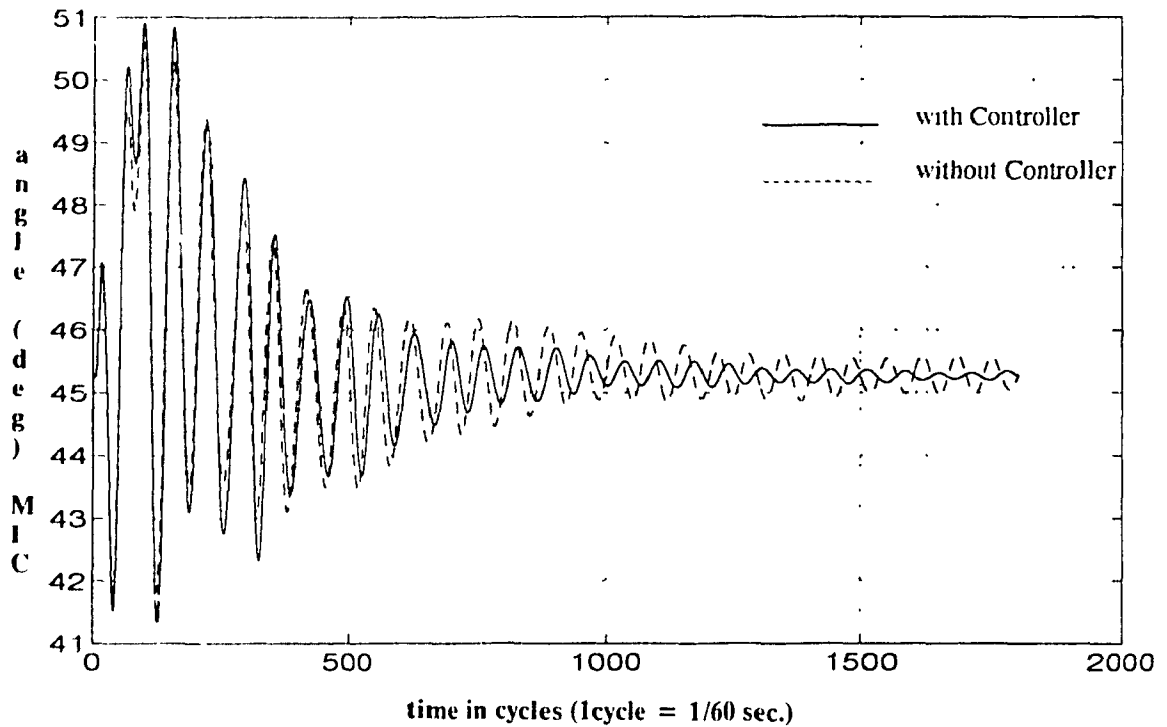
Figure 5.3 Machine angles (with ref. to MAU3) for machines at MIC (with SVC plus frequency input supplementary control and with SVC alone)

The results presented above show that addition of frequency input supplementary controller is able to increase the damping of oscillations observable in the frequency signal between the machines in the load area and set of machines located in the major generating station located at a distance of 1000 kms. However the important point to be highlighted is that this controller has a little negative effect on the machine oscillations between the LG and CHU. These results are presented in the fig 5.4 where it can be seen that the angular difference between these two set of machines(represented by broken lines) has increased. The damping of this mode requires the second controller designed specifically for this mode as described in the chapters 3 and 4. The results for the same are presented in the following section.
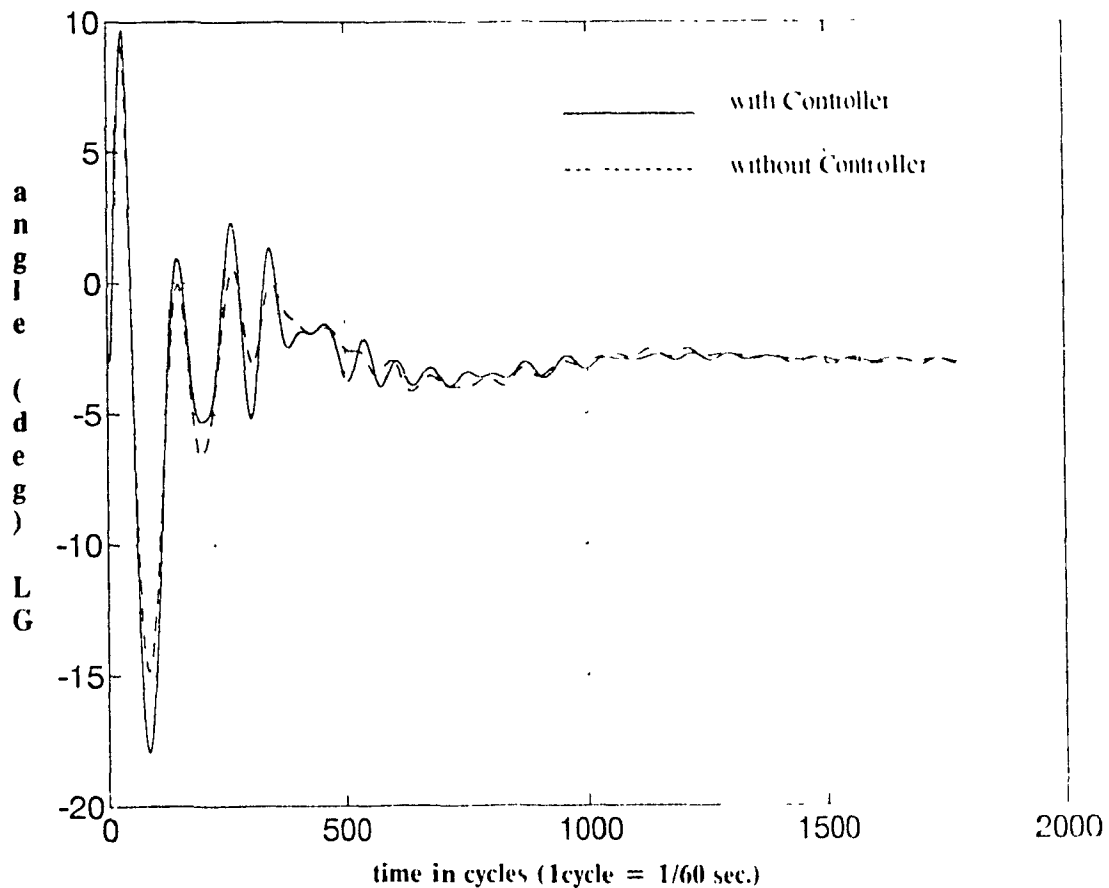
Figure 5.4 Machine angle between LG and CHU

2) LG-CHU Swing Mode oscillation

The signal used for this study was angular difference between LG and CHU itself. As discussed in chapter 4, it was observed during the design procedure that the rating of the SVC at the bus LVD7 had to be of sufficiently high value to enable it to exert certain significant influence on the first few peaks. The rating of SVC used for all the tests described above was 319 Mvars. However for this mode an additional unit of SVC was added resulting in total of 638 Mvars.
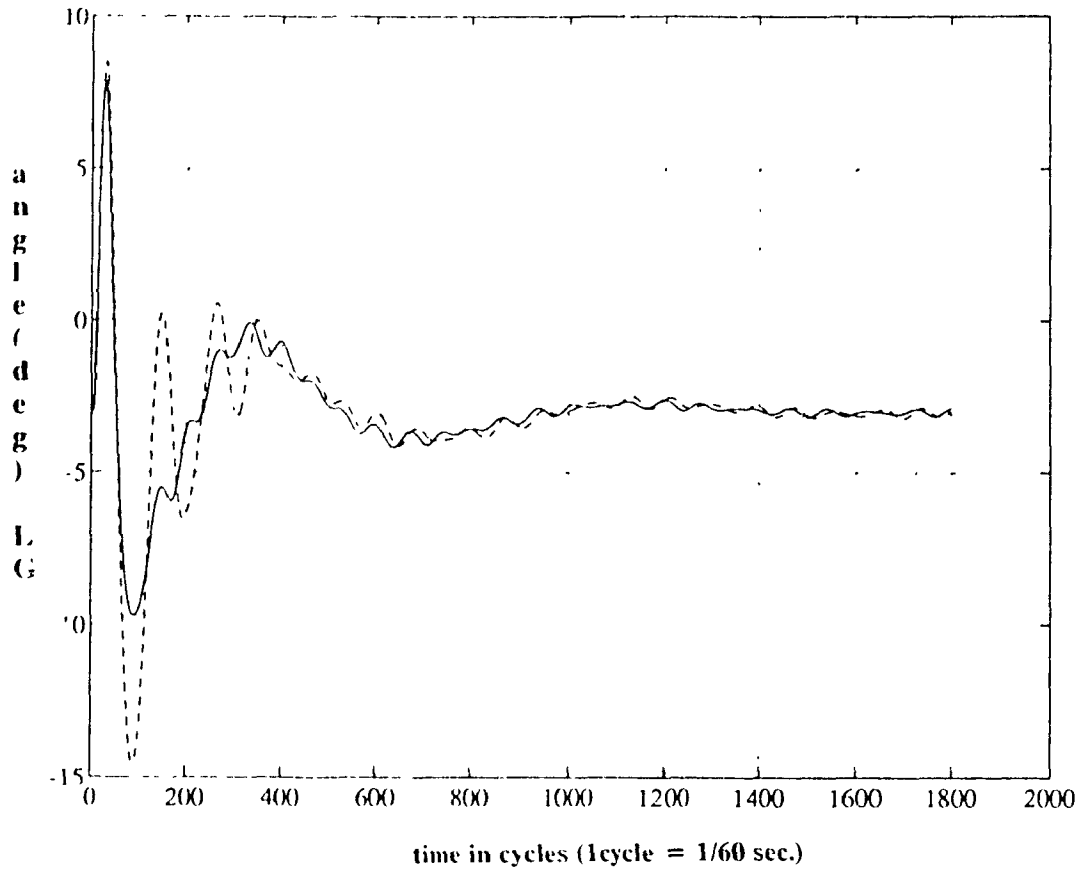
Figure 5.5 Machine angle between LG and CHU for SVC rated 638 Mvar with and without the LG–CHU swing controller

The test cases were run initially with this increased rating of SVC and then with SVC plus the angle input supplementary controller. The results are as shown in the figure 5.5 for SVC rated 638 Mvars and for comparison purposes figure 5.6, 5.7 show results for 319 and 1276 rating.
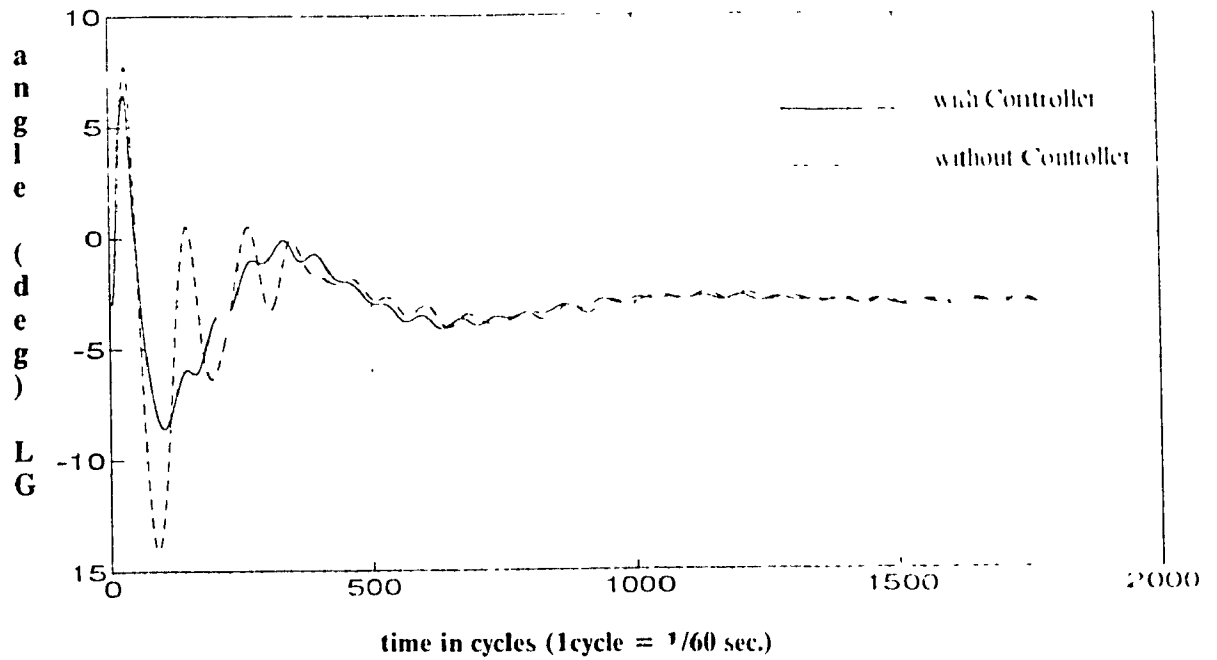
Figure 5.6 Machine angle between LG and CHU for SVC 1276 Mvar
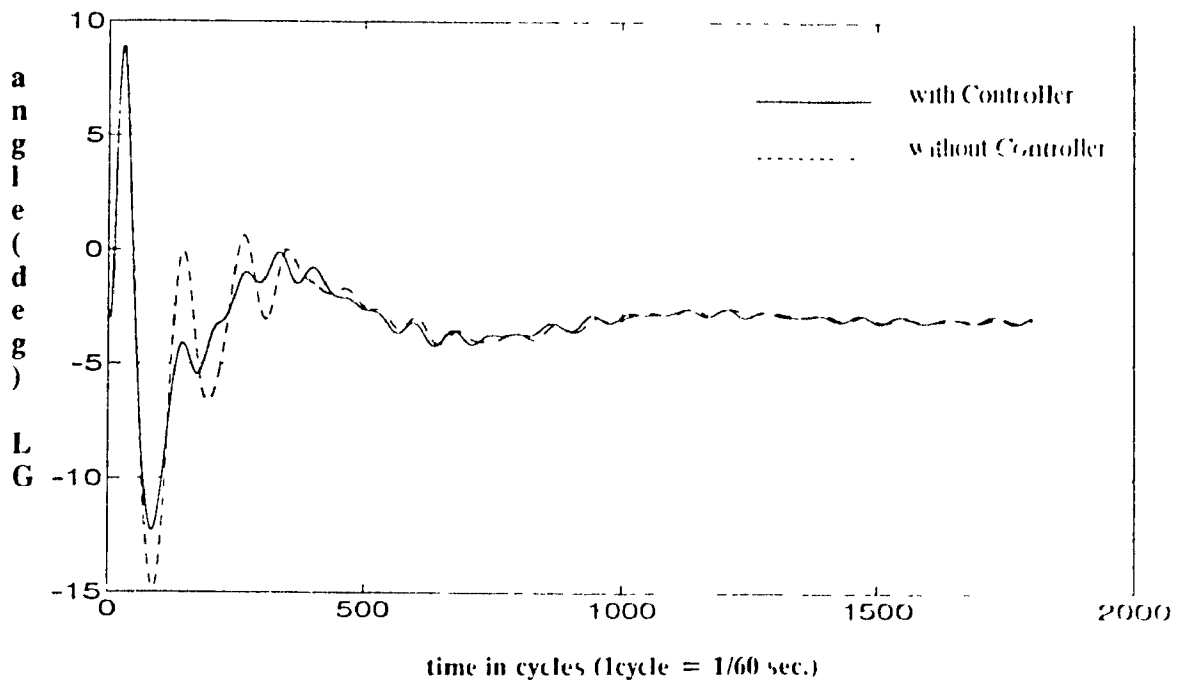
Figure 5.7 Machine angle between LG and CHU for SVC 319 Mvar

71

The addition of this control had very little opposite effect on the modes observable in the frequency at the bus LVD7. The plot of output frequency at the bus for these two cases is shown in the figure 5.8
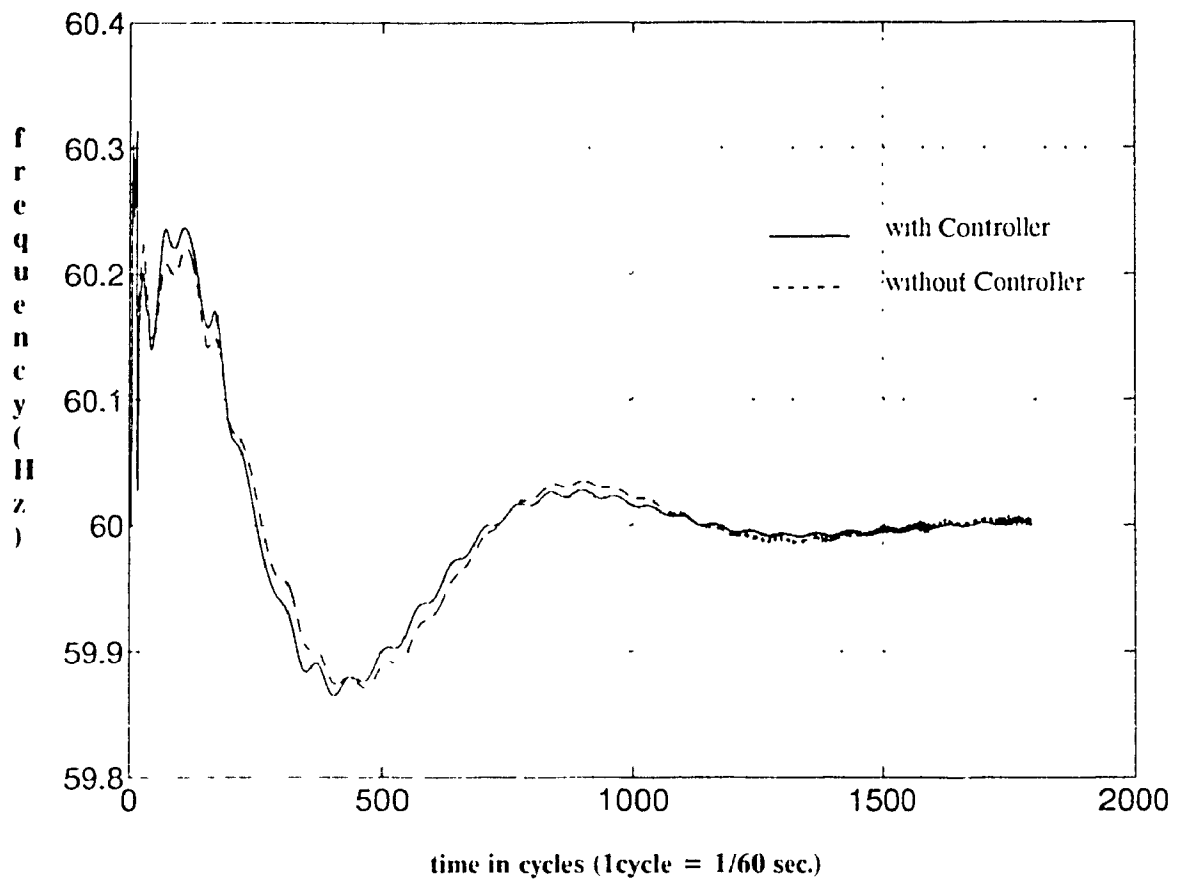
Figure 5.8 Output Frequency at LVD7 bus for 638 Mvar SVC.

The two set of controllers discussed are able to damp out the different modes of oscillations which may or may not be present in the locally available variables. The choice of mode to be damped will depend on the system conditions and requirements. It was also obseved that one type of controller designed and optimsed

for a particular input may have no or a little negative effect on the other modes. In case the requirement demands that several modes be damped from one SVC, it may require the controllers to work in parallel.

CHAPTER 6

SUMMARY, CONCLUSIONS AND FUTURE WORK

6.1   Summary

The approach presented in this thesis provides a method for designing a supplementary control to a SVC for damping of electro-mechanical oscillations using load modulation

As described in the chapter 2 following any disturbance, there are n−1 intermachine oscillations set up, where n is the number of the machines in the system. There also exists an n'th mode which represents the swing of all the machines in the system against the load.

These two modes as mentioned above are quite distinct and different in frequency The load or system mode oscillation is upto 0.1 Hz while the intermachine oscillations vary form 0.1 to 2.0 Hz.

An analysis was performed on a simple system comprising of 2 machines feeding into the load to determine the influence of the load modulation on intermachine swings. The location of controller was limited to the places where SVC's are already present in the system. However a sensitivity analysis was carried out to determine which one of the existing SVC's can be most effective for load modulation. Based on the results of this analysis, the SVC at bus LVD7 was chosen.

To be able to effectively damp out these modes, the question of controllability and observability comes up. Few of the modes which are observable in the frequency could be easily damped by using this signal as feedback and this was demonstrated. The modes which were not observable in the local signals available on the bus could also be damped if required feedback signal at the controller could be constructed with the help of communication. This was demonstrated by damping swings between machines at LG – CHU. This will result in supplementary loops in parallel with their output summed up before being fed into the summing junction of the SVC.

To determine the parameters of the controllers mentioned above a reduced order model representing the full system was identified. In the identification process for the reduced order model, the response of the system to a limited disturbance was considered as it resulted in linear relationship between susceptance B and deviations in frequency and voltage. A block of transfer functions was built which gave the similar response in terms of voltage and frequency when subjected to a pulse of B. An other block was also built to represent the change in B to changes in machine angle between LG and CHU.

These blocks were built in the Matrix$_x$ environment and the utilized to determine the various parameters like time constants and the gain to be used in the

75

feedback circuits. These parameters were found using root-locus method and by simulation (using Matrix$_x$ software package).

The values once finalized were verified using Hydro-Quebec's transient stability program on a network similar to Hydro-Quebec with 20 generators, (total generating capacity of 29,000 MW), 2 synchronous condensers, 3 SVC's , thirty 735 kV, twenty 315 kV buses and eight representing voltage level from 230 to 120 kV. A special subroutine was written representing SVC plus the controller and interfaced to stability program.

The results presented here clearly demonstrate the usefulness of these controllers for damping low frequency oscillations.

6.2 Conclusions and Future Work

The results show the usefulness of these controllers for increasing the damping of intermachine and system oscillations present in a power system. This increase in damping is a result of controlled load modulation which can be effectively carried out by proper placement of a SVC plus supplementary controller. It was also demonstrated that damping can be increased for the intermachine modes which may not be locally available on the SVC bus. However there are many areas highlighted below which need to be examined and further research carried out.

Further analysis might reveal that the swing oscillations not observed in the frequency are known and exist in some other signal available on the bus, then this information could be extracted from the other signal for example like branch power entering the control bus thus eliminating the need for remote communication

The controllers designed above are of fixed type and are useful for operating conditions which result in similar mode of oscillations and their usefulness may be limited if the operating conditions change resulting in different modes. This area can be avoided by making these controllers adaptive, so that the controllers can change the values of feedback time constants and gain parameters depending on the system operating conditions

77

REFERENCES

1) W. G. Hefforn and R. A. Phillips, " Effect of Modern Amplidyne Voltage Regulators on Underexcited Operation of Large Underexcited Operation of Large Turbine Generators ", *AIEE trans. (Power Apparatus and Systems)*, Vol. 71, pp. 692-697, August 1952.

2) F. P. deMello, C. Concordia, "Concepts of Synchronous Machine Stability as Affected by Excitation Control", *IEEE Trans on Power Apparatus and Systems*, Vol. PAS-88, No. 4, pp. 316-329, April 1969.

3) Bollinger, K. A Laha, R. Hamilton, T. Harras, "Power Stabilizer Design using Root locus Methods ", *IEEE Trans on Power Apparatus and Systems*, Vol. PAS-94, no. 5, September/October, 1975.

4) Rusche, P. A , D. L. Hackett, D. H. Baker, G. L. Gareis, P. C. Krause, "Investigation of the Dynamic Oscillations of the Ludington Pumped Storage Plant ", *IEEE Trans on Power Apparatus and Systems*, Vol. PAS-99, No. 6 November/December 1976, pp. 1854 1862

5) Kimbark, E W , Power System Stability Vol. I and III, John Willey and sons Inc., New York, 1956.

6) L Gyugyi, R A Otto, and T H Putman, "Principles and Applications of Static Thyristor Controlled Shunt Compensators", *IEEE Trans on Power Apparatus and Systems*, Vol PAS 97 No 5, pp 1935-45, Sept Oct 1978

7) D. McGillis, N. Hieu Huynh, G. Scott, " The Role of Static Compensation in Meeting AC System Control Requirement with Particular Reference to the James Bay System ", *IEE Proc. Generation, Transmission and Distribution*, 1981, 128, (6), pp. 389–393.

8) R. Elsliger, Y. Hotte, J. C. Roy, " Optimisation of Hydro-Quebec's 735 kV Dynamic Shunt Compensated System Using Static Compensators on a Large Scale ", *IEEE PES, Winter Power Meeting, New York*, Paper No. A78, 107–5, 1978

9) L. Gyugyi and E. Taylor, "Characteristics of Static Thyristor-Controlled Shunt Compensators for power Transmission System Applications", *IEEE Trans Power Ap par. and Syst.*, Vol. PAS–99, No. 5, pp. 1795–1804, 1980.

10) A. Olwegard, K. Walve, Gl Waglund, H. Frank, and S. Torseng, "Improvement of Transmission Capacity by Thyristor Controlled Reactive Power", *IEEE 1981 Power Engineering Society Winter meeting*, paper No. 81 WM 092 6, Feb., 1981

11) J. F. Hauer, R. I. Cresap, "Measurement and modelling of Pacific AC Intertie Response to Random Load switching", *IEEE Trans Power Appar and Syst*, Vol PAS–100, no. 1, January 1981.

12) E. V. Larsen, D. A. Swann, "Applying Power System Stabilizers Part I, II and III *IEEE Trans. Power Appar and Syst*, Vol PAS–100, No 6, June 1981

13) IEEE Committee Report, "Computer Representation of Excitation Systems , *IEEE Trans on Power Apparatus and Systems*, Vol. PAS 87 June 1968, pp. 1460 1461

14) R. T Byerly, D. I. Poznaniak and E. R. Taylor, "Static Reactive Compensation for Power Transmission Systems", *IEEE 1982 Power Engineering Society Winter Meet ing* Paper 82 WM 179 0, New York, January 31 February 1982 (Published II I I PAS, Vol PAS–101, pp 3997 1005, October 1982)

15) Task Force on Terms and Definitions, System Dynamic Performance Subcommittee, "Proposed Terms and Definitions for Power System Stability", *IEEE Trans Power Appar and Syst*, Vol. PAS-101, no. 7, July 1982.

15a) T. J. E. Miller, Editor, "Reactive Power Control in Electric Power Systems", John Wiley & Sons, New York, 1982.

16) J. F. Hauer, " Power System Identification by Fitting Structured Models to Measured frequency Response ", *IEEE Trans. Power Appar. and Syst.*, Vol. PAS-101, no. 4, April 1982.

17) A. L. Hammad, M. EJ-Sadek, "Application of a Thyristor Controlled Var Compensator for Damping Subsynchronous Oscillations in Power Systems", *IEEE/PES Summer Meeting*, Paper 83 SM 443-9, Los Angeles, California, July 17-22, 1982.

18) Symposium on Synchronous Machine Modeling for Power System Studies, *IEEE Power Engineering Society 1983 Winter Meeting*, February, 1983.

19) A.E .Hammad, "Analysis of Power system Stability enhancement by Static Var Compensator", *IEEE Transactions on Power Systems*, Vol. PWRS-1, No. 4, November 1986.

20) R.M. Mathur, Editor, "Static Compensators for Reactive Power Control", Canadian Electrical Association, Montreal, 1984

21) E Ohyamma, K Yamshita, L Maeda, H Suzuki and S. Mine, "Effective Application of Static Var Compensators to Damp Oscillations", *IEEE PES, Summer Meeting*, Paper No 84 SM 587-2,1984 also *IEEE PAS*, Vol. PAS-104, No. 6, pp. 1405-1410, June 1985

22) L. A. Enmez, (Editor), "Static var compensators", working group 38-01, task force No 2 on SVC, CIGRE, 1986

23) J.F Hauer, "Reactive Power control as a means for enhanced Interarea Damping in the Western US Power System   A Frequency Domain Perspective Considering

Robustness needs", *Application of Static Var Systems for System Dynamic Performance, IEEE Special Publication*, 87 TH0187-5-PWR, 1987, pp. 79-82

24) P. Czech, G. Scott, "Application of Static Var Compensators on Hydro Quebec's EHV System", Symposium on *Application of Static Var Systems for System Dynamic Performance, 1987, IEEE/PES 1987 Winter Meeting, Special Publication*, Paper 87TH0187-5-PWR.

25) L. Gyugyi, "Fundamentals of Thyristor-Controlled Static Var Compensators in Electric Power System Applications", *Application of Static Var Systems for System Dynamic Performance*, Special Publication No. 87 TH0187-5-PWR, San Francisco, CA, Jul. 15 1987, *IEEE Power Engineering Society Summer Meeting*, 1987, pp. 8-27

26) A .E. Hammad, "Applications of Static Var Compensators in Utility Power Systems", Application of Static Var Systems for System Dynamic Performance, Special Publication No. 87 TH0187-5-PWR, San Francisco, CA, Jul. 15, *IEEE Power Engineering Society Summer Meeting*, 1987, pp. 28-35.

27) R. M. Hamouda, M. R. Iravani, R. Hackam, "Coordinated Static Var Compensators and Power System Stabilizers for Damping Power System Oscillations", *IEEE 1987 Power Engineering Society Winter Meeting*, Paper 87 WM 015-8, New Orleans, Louisiana, Feb 1-6, 1987 (Published in *IEEE Trans Power Syst*, Nov 1987, pp 1059-1067).

28) L. V. Larsen, J. H. Chow, "SVC Control Design Concepts for System Dynamic Performance", Symposium on Application of Static Var Systems for System Dynamic Performance, 1987, *IEEE/PES 1987 Winter Meeting Special Publication*, Paper 87TH0187-5-PWR

29) D. L. Martin, "SVC Considerations for System Damping", Application of Static Var Systems for System Dynamic Performance *IEEE Special Publication No 87 TH0187-5-PWR*, 1987 pp 68-71

30) J. R. Smith, D. A. Pierre, D. A. Rudberg, R. M. Johnson, "Robust Var Unit Control Strategies to Enhance Damping of Power System Oscillations", Proceedings, *IASTED Conference on High Technology in the Power Industry*, pp. 238-243, March 1988.

31) J. R. Smith, "Robust Var Unit Control Strategies for Damping of Power System Oscillations", Ph.D Thesis, Montana State University, Bozeman, MT, July 1988.

32) K. P. Poon, K. C. Lee, "Analysis of Transient Stability Swings in Large Interconnected Power Systems by Fourier transformation", *IEEE transactions on Power Systems*, Vol. 3, No. 4, November 1988.

33) H. M. A. Hamdan, A. M. A. Hamdan, B. Kahhaleh, "Damping of Power System Oscillations by Excitation Control Using a Current Feedback Signal", *IEE Proceedings*, Vol. 136, Pt. C, No. 3, May 1989.

34) A. J. P. Ramos, H. Tyll, "Dynamic Performance of a Radial Weak Power System with Multiple Static Var Compensators", *IEEE Power Engineering Society Winter Power Meeting, New York*, 89 WM 183-5 PWRS, January/February 1989.

35) J. F. Hauer, C. J. Demeure, L. L. Scharf, " Initial results in Prony Analysis of Power System Response Signals ", Paper No. 89 SM 702-2 PWRS, *IEEE Summer Power Meeting, California*, July 9-14, 1989.

36) J. F. Hauer, " The use of Prony analysis to determine Modal Content and Equivalent Models for Measured Power System Response ", Panel Session on Eigenvalues and Frequency Domain Methods for system Dynamic Performance, *IEEE Summer Power Meeting, California*, July 9-14, 1989.

37) L. A. Hithy, M. A. Choudhary, " Effect of Load Models on AC DC System Stability and Modulation Control Design ", *IEEE Transactions on Power Systems*, Vol. 4, No. 2, May 1989

38) P. Kundet, M. Klein, G. J. Rogers, M. S. Zywno, "Application of Power System Stabilizers for Enhancement of overall System", *IEEE Transactions on Power Systems*, Vol. 4, No. 2, May 1989.

39) K. E. Bollinger, A. E. Mistr Jr., " PSS Tuning at the Virginia Electric and Power Co. Bath County Pumped Storage Plant ", *IEEE Transactions on Power Systems*, Vol 4, No. 2, May 1989.

40) N. Martins, L.T. G. Lima, "Determination of Suitable Locations for Power System Stabilizers and Static Var Compensators for Damping Electromechanical Oscillations in Large Scale Power Systems", 16th Power Industry Computer Applications Conference.Seattle, W.A, May 1–5, 1989 (Published in The Proceedings of *The 1989 Computer Applications Conference*, 1989, pp. 74–82)

41) J. R. Smith, D.A Pierre, I. Sadighi, M. H. Nehru, J. F. Hauer, "A Supplementary adaptive Var Unit Controller for Power System Damping", *IEEE Power Engineering Society Winter Meeting*, Paper 89 WM 197-5, New York, New York, Jan 29 Feb. 3, 1989.

42) D. J. Trudnowski, J. R. Smith, T A. Short, D A. Pierre, " An Application of Prony Methods in PSS Design for Multimachine Systems ", *IEEE Power Engineering Society Winter Meeting*, Paper 90 WM 117-2 PWRS, 1990.

43) E. Lerch, D. Povh, I. Xu, " Advanced SVC Control for Damping Power System Oscillations ", *IEEE Power Engineering Society Summer Meeting*, Paper 90 SM 160 6 PWRS 1990.

44) L Gerin-Lajoie, G Scott, E. V. Larsen, D. H Baker, A I. Imece, Hydro Quebec Multiple SVC Application Control Stability Study" *IEEE/PES 1990 Winter Meeting*, Paper 90 WM 082 2 PWRD, Atlanta, Georgia Feb 4 8 1990

45) J F. Hauer, ' The use of Prony Analysis to determine Modal Content and Equivalent Models for Measured Power System Response Presented at period seminar on

Eigenvalues and Frequency Domain Methods for System Dynamic Performance, *IEEE Power Engineering Society Winter Meeting 1990.*

45) M. Klein, G. J. Rogers, P. Kundur, "A Fundamental study of Inter area Oscillations in Power Systems", *IEEE PES 1991 Winter Meeting*, Paper 91 WM 015 8 PWRS

47) K. R. Padiyar, R. K. Varma, "Damping Torque Analysis of Static VAR System Controllers", *IEEE Trans. on Power Systems*, Vol. 6, No. 2, May 1991

48) P. M. Anderson and A. A. Fouad, "Power System Stability and control" Iowa state University Press, Ames, Iowa, 1982.

49) B. C. Kuo, "Automatic Control Systems", Prentice-Hall Inc., New York, 4th Ed., 1988.

50) W. D. Stevenson, "Elements of Power System Analysis", McGraw Hill, Inc 1982.

51) K. Ogata, "Modern Control Engineering", Prentice-Hall Inc., New York, 2nd Ed., 1990.

52) K. C. Lee, "Analysis of Power System Stabilizers Application for Controlling Poorly Damped Oscillations in the Alcan/B.C. Hydro Power Systems", *IEEE/PES 1992 Winter Meeting*, Paper 92 WM 163-6 PWRS

53) E. Z. Zhou, "Application of Static Var Compensators to Increase Power System Damping ", *IEEE/PES 1992 Winter Meeting*, Paper 92 WM 164 4 PWRS.

54) R. T. Byerly et al., "Normal Modes and Mode Shapes Applied to Dynamic Stability Analysis ", *IEEE Transactions on Power Apparatus and Systems*, Vol. PAS 94, no 2, March–April 1975.

55) S. B. Crary, "Power System Stability ", Vol. 1 and 2, Wiley, New York, 1945, 1947

56) L. Gerin-Lajoie, D. McGillis, G. Scott, "Static Compensator Applications and their limitations" *International Symposium on Electric Energy Conversion in Power systems*, Capri, Italy May 1989

APPENDIX A

System transfer function

The transfer functions defined below represents the functions used for designing the controller for damping of low frequency oscillations observed in the frequency signal at bus LVD7.

$$\frac{n_1}{d_1} \quad \frac{2.49}{3.0S^2 + 0.935S + 0.5429}$$

$$\frac{n}{d} \quad \frac{2.15}{3.0S^2 + 0.15S + 93.168}$$

$$\frac{n}{d} \quad \frac{0.2723S + 0.092}{1.15S + 0.2}$$

$$\frac{n_1}{d_1} \quad \frac{8.63}{3.0S^2 + 4.71S + 18.5}$$

$$\frac{n}{d} \quad \frac{9.9362}{3.15S^2 + 24.03S + 81.02}$$

APPENDIX B

Subroutine Interfaced to Stability Program

SIC01

Static compensator model with supplementary signal

The following appendix describes the program written and interfaced to the in house stability program (ST600) at IRE Q. The block diagrams corresponding to this program are given in figure 3.10 (chapter 3) and figure 4.6 (chapter 4).

P,TM,0.005

P,K,2.85

P,VLMAX,0.10

P,VLMIN,-0.10

P,KP,33.33

P,TC,0.12

P,DMAX,1.0

P,DMIN,-1.0

P,T1,3.50

P,T2,0.01

P,T3,0.100

P,T4,0.50

P,T5,0.09

P,T6,0.0005

P,T7,0.0005

P,T8,0.0005

P,T9,0.0005

P,T10,0.0005

P,TDEL,0.0005

P,AMAX,1.0

P,AMIN,-1.0

P,PCt,6.283185

P,J1,0.20

P,J2,.636

P,J4,1.0

P,Kb,.0001

Lecture des parametres du modele dans le fichier de donnees stabilite

PS1,ID,PUI,TM,NUM,T1,T2,T3,T4,T5,K,VLMIN,VLMAX

PS1,TC,DMAX,DMIN,XNOMC,JNOM,T6,T7,T8,T9,KP,AMAX,AMIN

Description des donnes :

ID	:	numero du barre
PUI	.	static compensator base power (MVA)
TM	:	measurement time constant
T1 - T9	:	lead lag phasing circuit time constant
VLMIN	·	minimum value for the other signal
VLMAX		maximum value for the other signal
TC		control time constant
DMIN		error value and tripping acceleration

DMAX   :   error value and tripping acceleration

KP   :   slope adjustment

AMIN   :   dynamic value of the compensator susceptance

AMAX   :   dynamic value of the compensator susceptance

TDEL   :   true delay due to thyristor response

XNOMC   :   bus number of the controlled bus (volt)

JNOM   :   bus number of the controlled bus (freq)

Identification du circuit

P,IDE,#ID(ID)

   Conditions initiales

P,FRO,OMEGA0(NUM)

P,VREF,VT0(XNOMC)

   calculation de autre signal

=,VRF1,VRF1

FREQ,FR,JNOM

=,FR11,FRO

+,DFR,FR,FR11,1.0,-1.0,1.0

+,DFR,DFRs,60,-1.0,0.0,0

DB,DFRs,DFRa,.0009

DER,DFRa,sx

DFR,sx,s2x

DER,y,sy

DER,sy,s2y

+,s2y,sy,y,s2x,J1,J2,J4,-J1,0.0

DER,y,DERE,T1

FILT,DERE,DFR1,1.0,T1

+,DFR1,DFR2,K,-1.0,0.0

=,VMIN,VLMIN

=,VMAX,VLMAX

TR,DFR2,DFR4,1.0,T2,1.0,T3

TR,DFR1,DFR2,1.0,T2,1.0,T3

+,DFR2,DFR4,K,-1.0,0.0

LIM,DFR4,DFR5,VMIN,VMAX

+,DFR8,DFR5,1.0,-Kb

   system calculations

TLNS,VTXNOMC

FILT,VTVT1,1.0,TM

+,VT1,VT2,DFR5,VREF1,1.0,1 0,1.0,-1.0,0.0

TR,VT2,VT3,1.0,T6,1.0,T7

TR,VT3,VT4,1.0,T8,1.0,T9

-,AMLAMIN

```
= ,AMA,AMAX

TRL,VT4,VT5,AMI,AMA,KP,0,1.0,TC

+ ,VER,VT,-1.0,1.0,1.0

EPS,VT5,VC,VER,DMIN,DMAX,AMIN,AMAX

TRL,VC,CB,AMI,AMA,1.0,0.0,1.0,TDEL

* *,VT,VB,2

        = ,VB,1.0

*,VB,CB,POWER,PUI

+ ,POWER,QR,1.0,1.0,0.0

    stability interface

QLB,QR,XNOMC
    report monitoring

RAPP,VT1,CB,POWER,VRE1,DER2,ER,DER,DER1,DER5,DER1,v,ER1
```

APPENDIX C

SVC modeling parameters

The parameters given below were used for modeling the static var compensator in the stability program (refer drawing 3.10).

Tm = 0.017 seconds

Kp = 33.33 (slope of 3%)

Tc = 0.12 seconds

T1 = 0.005 seconds

T2 = 0.005 seconds